eFRADIR: An Enhanced FRAmework for DIsaster Resilience

ALIJA PAŠIĆ[ID][1], **RITA GIRÃO-SILVA**[ID][2,3], **FERENC MOGYORÓSI**[ID][1], **(Member, IEEE)**,
BALÁZS VASS[ID][1], **(Graduate Student Member, IEEE)**, **TERESA GOMES**[ID][2,3], **(Member, IEEE)**,
PÉTER BABARCZI[ID][1], **(Member, IEEE)**, **PÉTER REVISNYEI**[ID][1], **JÁNOS TAPOLCAI**[ID][1],
AND JACEK RAK[ID][4], **(Senior Member, IEEE)**

[1]MTA-BME Future Internet Research Group, Department of Telecommunication and Media Informatics, Faculty of Electrical Engineering and Informatics (VIK), Budapest University of Technology and Economics (BME), 1111 Budapest, Hungary
[2]Department of Electrical and Computer Engineering, University of Coimbra, 3030-290 Coimbra, Portugal
[3]Institute for Systems Engineering and Computers at Coimbra (INESC Coimbra), 3030-290 Coimbra, Portugal
[4]Faculty of Electronics, Telecommunications, and Informatics, Gdańsk University of Technology (GUT), 80-233 Gdańsk, Poland

Corresponding author: Alija Pašić (pasic@tmit.bme.hu)

ABSTRACT This paper focuses on how to increase the availability of a backbone network with minimal cost. In particular, the new framework focuses on resilience against natural disasters and is an evolution of the FRADIR/FRADIR-II framework. It targets three different directions, namely: network planning, failure modeling, and survivable routing. The steady state network planning is tackled by upgrading a sub-network (a set of links termed the spine) to achieve the targeted availability threshold. A new two-stage approach is proposed: a heuristic algorithm combined with a mixed-integer linear problem to optimize the availability upgrade cost. To tackle the disaster-resilient network planning problem, a new integer linear program is presented for the optimal link intensity tolerance upgrades together with an efficient heuristic scheme to reduce the running time. Failure modeling is improved by considering more realistic disasters. In particular, we focus on earthquakes using the historical data of the epicenters and the moment magnitudes. The joint failure probabilities of the multi-link failures are estimated, and the set of shared risk link groups is defined. The survivable routing aims to improve the network's connectivity during these shared risk link group failures. Here, a generalized dedicated protection algorithm is used to protect against all the listed failures. Finally, the experimental results demonstrate the benefits of the refined eFRADIR framework in the event of disasters by guaranteeing low disconnection probabilities even during large-scale natural disasters.

INDEX TERMS Availability, disaster resilience, general dedicated protection, probabilistic failure, regional failure, spine, survivable routing.

I. INTRODUCTION

The changed user behaviour during the current pandemic highlighted the utmost importance of reliable communication networks and services, which support the increased traffic generated by, e.g., online teaching and home office. These new challenges of our digital society accelerated the prolif-

eration of mission-critical services, which highly depend on the performance of the underlying networks, in particular on the continuity of network connections. The availability and reliability of the communication infrastructure are usually quantified as Quality of Resilience (QoR) [1]–[3], which is expected to be very high for mission-critical services like telesurgery or stock market (even including additional latency constraints). These properties are not only determined by the underlying network infrastructure, but also by the proper

The associate editor coordinating the review of this manuscript and approving it for publication was Zhenzhou Tang[ID].

usage of resources and engineering, as well as the scientific knowledge to deploy communication paths for such services in a reliable manner.

Although cuts of network links during construction works are often the main cause for service outages in the Internet, operators of large transport networks may also face additional challenges, i.e., natural disasters owing to the national or continental scale of their networks [4]. However, today's communication networks are still designed to consider only single link [5] or dual link failures [6], and are not prepared for scenarios of disasters. Such a classical approach is clearly not sufficient to respond to the up-to-date requirements and challenges [4]. Therefore, the adequate failure modeling, network planning, and routing schemes and processes (i.e., protection mechanisms) can help us to create truly reliable networks and services, on which our society can rely, even in disastrous circumstances [4], [7].

Disasters are defined as significant network outages, where telecommunication equipment in a given area becomes non-operational. Disasters can occur due to manifold reasons, including natural events (such as earthquakes, floods, fires, hurricanes, tsunamis, tornadoes, etc), human errors (i.e., technical errors that may result in cascading failures) or even malicious attacks (hacking, electromagnetic pulse (EMP) attacks, or the use of weapons of mass destruction (WMD)) [4], [8]. In particular, natural disasters often affect seriously the performance of communication networks by leading to failures of multiple nodes/links located in disaster areas.

An increasing frequency of disaster-related massive failures observed over the last two decades magnifies the importance of the problem [4]. Therefore, to guarantee the high availability required by numerous network services (a common availability requirement is the "five-nines", i.e., 0.99999), it is crucial to apply resilience mechanisms able to assure the adequate protection and fast recovery in disaster scenarios. Thus, for no surprise, disaster-resilience of communication transport networks raised significant interest [8]–[10].

Natural disasters are often modeled by *regional failures*, and they can have different sizes and shapes, as illustrated in Fig. 1. Regional failures per definition correspond to a joint failure of nodes/links located in the considered affected geographic area [11]–[13], which form different sets of *Shared Risk Link Groups* (SRLGs). Most of these failure modeling approaches seek to find the proper trade-off between the accuracy and state-space explosion (i.e., the number of SRLGs). Note that, if the topology provides some basic connectivity even after regional failures, the number of SRLGs can be reduced in these models, while their accuracy is maintained. Therefore, jointly considering independent single link failures for a reliable topology design and SRLGs to find disaster-resilient paths for the connections would further improve the availability perceived by the end-user.

To the best of our knowledge, the FRAmework for DIsaster Resilience (*FRADIR*), originally introduced in [14], is the
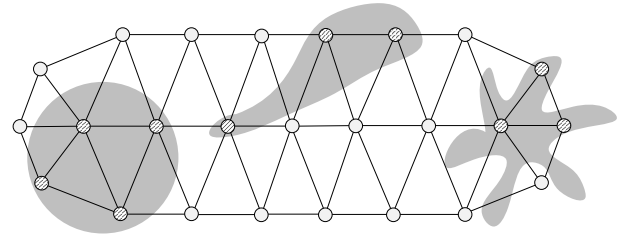

FIGURE 1. Examples of failure regions marked in grey: a circular failure region characteristic, e.g., to an earthquake (the left region), and irregular failure regions, e.g., due to a hurricane, flood (the middle region) or a volcano eruption (the right region).

first framework that jointly utilizes failure modeling, network planning, and survivable routing to ensure disaster resilience. In [14], it was shown that planning the network merely for the steady state is not sufficient since disasters would disconnect the network very frequently. Hence the framework was further refined in [7] by introducing novel failure modeling and network planning components. In the refined FRADIR-II framework [7], independent random failures and regional failures were jointly considered to model the effect of disasters. First, an infrastructure was designed against random failures, termed as *the spine*, which guarantees a certain availability to the working paths (WPs). In a second step built on the SRLG concept[1] to model disaster-caused outages, a probabilistic regional failure model [16] was applied, where a modified Euclidean distance of an edge to the epicenter of a disaster was used to generate a failure list, which is deemed to be more realistic than previous approaches. Based on the generated list, a link upgrade strategy was proposed attempting the reduction of the likelihood of the regional failures in the list disconnecting the network. Finally, the generalized dedicated protection approach was used to route the connections [17].

Although FRADIR/FRADIR-II demonstrated the benefits of jointly considering network planning, failure modeling, and survivable routing against disasters, there was still room left for further improvements in all dimensions of the framework (e.g., in the rigid pre-defined link upgrade steps dependent on the topology). Hence, in this paper, we fine-tuned these aspects and improved all steps with the state-of-the-art models and algorithms to obtain a comprehensive approach against disasters and make its application easier for network operators.

A. MAIN CONTRIBUTIONS AND PAPER ORGANIZATION

In our current paper, we further improve the previously introduced FRADIR-II framework in several aspects (e.g., the cost of network upgrade and routing, or the algorithm running time) to get more accurate disaster models and algorithms, which help to meet the requirements of mission-critical communication services.

---

[1]An overview of progress in standardization related to information and communication technology for disaster relief systems, network resilience, and recovery by the ITU is given in [15].

TABLE 1. Examples of massive failures due to natural disasters.

Year	Type	Area of impact	Consequences for communication networks
2005	hurricane Katrina	USA	long-lasting massive failures of nodes due to power supply faults
2006	earthquake (magnitude of 7.1)	Taiwan	failures of seven submarine optical cables; connectivity between North America and Asia disrupted for several weeks
2011	Greatest Japan Earthquake of 9.0 magnitude	Japan	failures of undersea optical links; about 1,500 telecom switching offices affected
2017	hurricane Maria	Latin America, Mexican Gulf	no cellular communications in Puerto Rico (in 95%) and in Dominicana; no Internet in Dominicana
2018	Attica fires	Greece	communications in the affected areas hardly possible
2020	cyclone Amphan	Eastern India	cuts of about 100 fiber links by falling trees due to wind (at nearly 200 km/h); reduction of the available network capacity down to 65-70% in the affected areas

Apart from highlighting the related works and the evolution of FRADIR schemes in Section II and Section III, the list of our contributions presented in this paper forming the basis of the proposed eFRADIR model introduced in Sections IV-VI includes:

1) the enhanced spine selection approach described in Section IV that allows obtaining the results in a short time for large networks. In particular, it is a two-stage approach, where in the first stage an adaptation of previous heuristics is considered,

2) a novel complex earthquake activity and magnitude-based failure model founded on the earthquake activity rates and the relation between the magnitude and the size of a disaster area, resulting in a more comprehensive model, compared to the most commonly used ground-shaking hazard models (Section V). Furthermore, compared to the former versions of FRADIR, we improve the coupling of the independent random failures and regional failures in our eFRADIR framework,

3) introduction in Section VI of a novel Integer Linear Program (ILP) for the disaster-resilient network planning for optimal link upgrades followed by the presentation of heuristic schemes to reduce the running time.

Experimental results are presented in Section VII to illustrate the advantages of eFRADIR. The paper is concluded in Section VIII.

II. RELATED WORK

In this section we present some of the recent disaster-related massive failures and their effect on communication networks (Section II-A), and the related work concerning different aspects of our framework (Section II-B).

A. MASSIVE FAILURES AND CONSEQUENCES

The consequences of natural disasters are often severe and the time needed for a physical repair of the failed network elements is frequently significant as the area itself is typically remarkably damaged (e.g., by floods, fires). Also, the failed network elements (such as undersea links) are often not easily accessible. The impact of selected natural disasters on networks is presented in Table 1.

For instance, hurricane Katrina in 2005 triggered power outages resulting in failures of network nodes lasting for over ten days [18] and the degradation of the average network availability down to 85% [19]. The earthquake in 2007 in Taiwan with the magnitude of 7.1 resulted in failures of seven undersea optical links interrupting the Internet connectivity between Asia and North America as well as communications to China, Hong Kong, Japan, Korea and Singapore for weeks [9], [20]. The Greatest Japan Earthquake in 2011 with the epicenter in the ocean area near Japan apart from causing failures of submarine optical links, was responsible for outages of 1,500 telecom switching offices in Japan [21], [22]. Hurricane Maria in 2017 in Latin America, in turn, caused the country-wide collapse of cellular communication systems in Puerto Rico and Dominicana, as well as prevented from Internet communications in the affected areas [23]. Fires occurring in Greece in 2018 (and in several other Mediterranean countries) burned many wired links and suspended communications in the impacted regions [24]. Cyclone Amphan in Easter India caused massive failures of about 100 optical links installed over the ground due to the falling trees and reduced the available network capacity down to 65-70% in the affected areas [25].

Examples of unintentional human faults at the hardware maintenance or software level leading to simultaneous massive failures often regarded as technology-related disasters [26] include, e.g., an outage at Google in August 2013 (which, although lasting for only 5 minutes, resulted in a reduction of the Internet traffic worldwide by about 40% [27]), an outage at Amazon on February 28, 2017 bringing about the S3 service disruption in the US-EAST-1 region [28], or the intermittent connectivity at Microsoft Cloud on September 11, 2019 [29].

Massive failures in communication network resulting from intentional human activities (attacks) include either direct activities such as EMP attacks [30], or distributed denial of service (DDoS) attacks (see, e.g., an attack in 2018 targeted at GitHub by malicious traffic at 1.35 Tbps [31]), as well as the indirect results of, e.g., bombing, or use of WMD – not primarily targeted at communication networks [32].

B. SURVIVABLE NETWORK AND CONNECTION DESIGN

Network failure modeling is not directly contributing to enhancing disaster resilience. Nonetheless, it is a key aspect since it is crucial to model the environment and network

properly, and hence it is a widely studied topic [11]–[13], [22], [33]–[37]. In [11], [22], [38]–[40] the impact of natural disasters on terrestrial links and in [20], [41] the impacts on submarine cables are investigated thoroughly. In [42], a greenfield (i.e., planning from scratch and not extending any existing network) fault-tolerant network design approach was introduced, which is based on a new metric called multiple region-based connectivity that describes multiple massive localized faults (i.e., multiple regional failures). In [43], the concept of emergency optical networks and hierarchical addressing was reviewed as a strategy to enhance optical network resilience against disasters. In [44], stochastic models and risk-minimizing node relocation schemes were suggested aimed at planning new locations for nodes to obtain a higher level of disaster-resilience.

On the one hand, resilience of the already deployed topologies against independent failures may be achieved by improving the network availability and reliability through the use of *network topology design* tools [45]–[48]. The definition of a high availability sub-graph at the physical layer, designated the *spine* in [49], may also play an essential role concerning the network resilience. The aim is to offer high availability services (in some cases, with other protection schemes) and more differentiated QoR classes [50], which makes this a suitable approach to support critical services. Another approach that may be considered for the enhancement of network robustness involves shielding some links, as in [51], however, without explicitly taking availability into account.

On the other hand, besides an upgraded topology, the perceived availability by the end-user can be improved with a careful connection design as well. *Survivable routing schemes* are used to improve the resilience of connections [52], often categorized by the time-scale and (bandwidth) cost when protecting against link failures [53], [54] and disasters [55]. In particular, the family of survivable routing algorithms known as General Dedicated Protection (GDP) [17], [56] ensures instantaneous failure recovery against any protectable failure pattern (given for example as an SRLG list). With the GDP approach, a minimum cost acyclic graph may be devised for a source–destination pair, ensuring connectivity in all considered SRLG failure scenarios, often resulting in better bandwidth efficiency than a disjoint path-pair [57] for sparse SRLG lists. The concept was later extended with algebraic operations to support network coding for resilience in scenarios of single link failures [58]–[60]. Geo-diverse routing can be utilized to increase network survivability to disasters as well by a spatial separation between disjoint paths [61]–[63] according to the pre-defined failure regions. Thus, it requires precise failure modeling. However, GDP can ensure service continuity in the presence of regional failures and complex SRLG lists as well (where a failure-disjoint path pair may not exist) as long as the network remains connected upon a failure (which may not always be the case for large-scale disasters).

It is worth noting that the state-of-the-art methods, presented in this section addressing the failure modeling, net-

work planning and survivable routing issues in the context of disasters, tackle these problems only separately. Indeed, none of them combines the merits of failure modeling, network design and survivable routing. In Section III we present the evolution of our FRADIR scheme which combines all three research areas to create a comprehensive flexible (i.e., tunable) framework which ensures disaster resilience.

III. EVOLUTION OF FRADIR

In Section III-A we introduce the initial concept of FRADIR, afterwards in Section III-B we give an overview of its development concerning the algorithms used in different aspects. Finally, in Section III-C we discuss our new approach i.e., eFRADIR.

A. OVERVIEW OF THE FRADIR FRAMEWORK

In the original FRADIR [14] framework, a combination of network design, failure modeling and survivable routing proved to be a good strategy to improve disaster resilience of mission-critical applications, in particular when compared to using only one of the methods at a time. FRADIR was also innovative in a sense that two different failure models were jointly considered: independent failures (such as cable cuts) and regional failures (i.e., disasters).

The *spine* concept was used in FRADIR to guarantee a minimal availability for all WPs. The spine is defined as a subgraph (not necessarily a spanning tree) consisting of elements used by WPs serving traffic requiring a higher level of availability (i.e., the highest resilience class). Backup paths (BPs) can, in turn, be set up using any of the links. In FRADIR, the WPs consisted of edges in the spine, whose availability was modified, if necessary. Therefore, a network with upgraded availability was achieved. An example is displayed in Fig. 2. In this figure, the spine is formed by network elements of improved availability, marked with thick lines, as opposed to the other elements of a ''nominal (i.e., lower)'' availability. There are several techniques to improve availability, such as hardware (e.g., more expensive network equipment), equipment siting (e.g., replace above-ground cabling with underground), or workforce training (e.g., assign the most experienced staff to the operations). For example, 60 km aerial cable has three-nines availability (8.77 hours expected downtime yearly). In contrast, the same cable buried in the ground would have four-nines availability (53 minutes expected downtime yearly) [64].

As we have seen, large-scale failures can be modeled with the help of SRLGs. An SRLG consists of a set of links that share a common resource (e.g., links sharing a fiber, a cable or a duct) or are simply physically close to each other, and hence are at risk at the same time concerning a given disaster event. A *regional failure modeling* method incorporating the upgraded link availability values by the spine was considered. A list of SRLGs representing failure events of probability higher than a specific value was devised. As the network was enhanced through the spine, the number of SRLGs was significantly reduced.
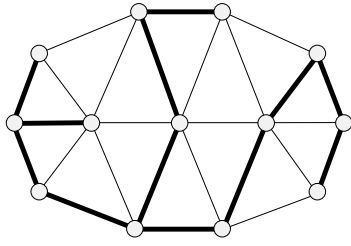
FIGURE 2. Example of the spine concept [49]: a higher availability elements marked with thick lines.

Afterwards, considering the generated SRLG list, a *survivable routing scheme* allowed for the improvement of the resilience of connections. For comparison, experiments with two different schemes, GDP with routing (GDP-R) [56] and SRLG-disjoint path pair (1+1 protection) were carried out. It was shown that the GDP-R always outperforms the 1+1 in terms of blocking probability and resource allocation. This is possible because the GDP-R minimizes the total bandwidth cost and provides the optimal solution for non-bifurcated flows. An often encountered problem was the disconnection of the network when considering regional failures, resulting in a non-protectable failure scenario. In [65] the availability routing cost trade-off of various routing methods was studied.

B. IMPROVED DISASTER RESILIENCE: FRADIR-II

The extension of FRADIR – namely FRADIR-II [7] – tackles the problem of non-protectable failures by considering a network design algorithm, which can identify and prevent possible network disconnections. Another aspect improved in FRADIR-II was the way the spine was devised, as a cost-based model was used (the spine was obtained so that a minimal availability was guaranteed for all WPs at a minimal availability upgrade cost).[2] The failure modeling technique was also improved in FRADIR-II by using a novel availability-based distance function of a link to the epicenter of a disaster (where the impact area of a disaster is assumed to have a circular shape). This way, a link with higher availability is represented as having a greater distance to the failure epicenter. Nonetheless, FRADIR-II still utilized a ground-shaking hazard model, which is less precise and realistic compared to the earthquake activity and magnitude-based model introduced by us in this paper for eFRADIR. In addition, FRADIR-II implemented a topology-dependent rigid pre-defined link upgrade method.

Furthermore, in FRADIR-II we compared two advanced protection schemes, namely the GDP with routing (GDP-R) [56] and the SRLG Diverse Routing (DR) [66]. Note that if not all links are included in the SRLG list, the DR does not guarantee two disjoint paths (as is often assumed). The 1 + 1 SRLG disjoint protection is a special case of DR when the

SRLG list includes all the links. It was shown that the GDP-R always outperforms the DR in terms of blocking probability and resource allocation.

A comparison of the characteristics of the previous frameworks (FRADIR/FRADIR-II) is presented in Table 2. The results obtained by FRADIR-II illustrated the trade-off between the average capacity consumption of the routing approach and the total upgrade cost. In particular, they showed that it is possible to decide whether to invest in the network upgrade (which will result in a lower routing cost) or not (which will entail a higher routing cost due to the need to protect against more complex failure scenarios). However, FRADIR-II still wasn't sophisticated enough to respond to extremely hard requirements of mission-critical applications in large network topologies.

C. ENHANCED FRADIR

In this paper, with proposing eFRADIR we make a remarkable progress towards a comprehensive connection resilience framework by further improving FRADIR-II. An overview of our concept is presented in Figs. 3-4.

In the *network planning phase*, we first design a spine infrastructure characterized by high availability. Although the previously used spine design approaches allowed to obtain optimal solutions, their running time made them applicable only in small- and medium-sized networks. Our novel two-stage spine approach introduced in Section IV makes eFRADIR applicable in large-scale networks as well. In the *failure modeling phase* in Section V, a novel complex earthquake activity and magnitude based regional failure model is discussed instead of the modified Euclidean distance of the previous FRADIR-II version. We propose a novel ILP as well for optimal link upgrades in Section VI, and improve existing heuristics to reduce the running time. Finally, we use GDP-R [56] to establish connections in a similar way as in the case of previous FRADIR and FRADIR-II versions.

Our approach is designed primarily for wide area networks as a remedy for the large-scale natural disasters often seriously affecting their performance. In this paper, we decided to present its general form (with a generic meaning of the demands) to make it a valid scheme regardless of the individual properties of a given network architecture. Therefore, concerning the common multilayer concept of communication networks [67], apart from its default application in the transport layer, our eFRADIR can be applied at the IP layer as well. For its application in a specific context (e.g., for wavelength-division multiplexing (WDM) transport networks [68] or elastic optical networks (EON)) [69], the individual properties of these architectures need to be further modelled. Typically, it would mean incorporating additional constraints referring, e.g., to wavelength continuity (often important in WDM networks), or spectrum continuity constraints (for EONs).

---

[2]Note that in FRADIR, no cost function was considered when devising the spine. However, the formulated linear problem was solved in FRADIR in an exact way, which is not scalable for larger networks.

TABLE 2. Comparison of the used methods in previous versions of the framework (FRADIR/FRADIR-II).

Components	FRADIR	FRADIR-II
Spine design	ILP for finding the spine (spanning tree) that maximizes the average availability of the WP for each demand	MILP for finding the spine (spanning tree) that guarantees a minimum value for the availability of each WP at a minimal cost
Failure modeling	Unavailability-based regional failure model, where the availability upgrade of the spine links affects the probability of the SRLGs directly	Availability-based regional failure model using a modified Euclidean distance (of an edge to the epicenter of a failure) that incorporates information on the availability of the edge
Link upgrade to prevent network disconnections	–	Heuristic algorithm which prevents network disconnections by upgrading the availability of links
Survivable routing	General Dedicated Protection with Routing	General Dedicated Protection with Routing
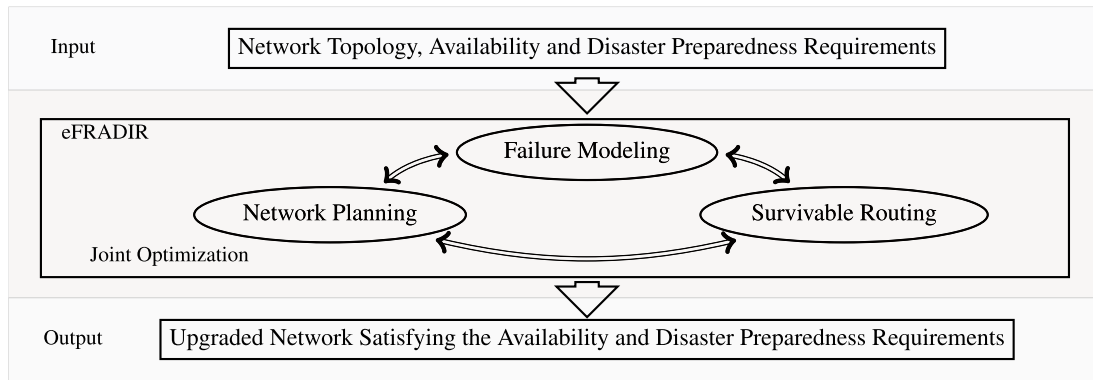
FIGURE 3. The high level concept of eFRADIR – the joint utilization of failure modeling, network planning and survivable routing is the key for proper disaster preparedness.
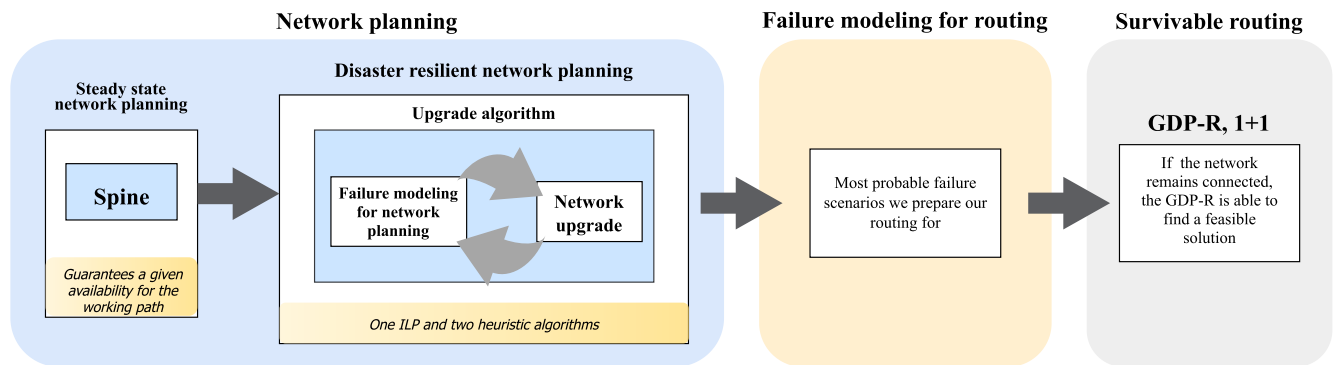
FIGURE 4. A detailed description of the eFRADIR framework.

IV. STEADY STATE NETWORK PLANNING PHASE

In this section, we introduce our network model and our spine design used by eFRADIR for resilient network planning against independent failures.

A. NETWORK MODEL

Throughout the paper, the network is represented by a graph $G(V, E)$ embedded on the Earth surface, where V is the set of nodes representing Optical Cross-Connects (OXCs) and E is the set of undirected edges, each edge e representing a bidirectional fiber connection between the OXCs with the corresponding routing cost $c(e)$ and availability $a(e)$ values. Each undirected edge may be represented by a pair of directed links in opposite directions pertaining to a set E_d. The position of each node is given by longitude and latitude coordinates. Each edge $e \in E$, has an initial availability value $a_0(e) \in [0, 1]$: $a_0(e) = 1 - \frac{MTTR}{MTBF(e)}$. The Mean Time To Repair ($MTTR$) a failure is considered as $MTTR = 24$ h

and the mean time between steady state random failures of e is $MTBF(e) = \frac{CC*365*24}{\ell(e)}$ [h]. The parameter CC denotes the cable cut metric, considered to be 450 km [50]. The unavailability of an edge e is calculated as $U(e) = 1 - a(e)$, with $a(e)$ being the (final) availability of the edge (it can be the initial availability $a_0(e)$ or a modified availability, as explained later). Note that the initial availability of an edge e is a function of its length, $\ell(e)$ [km], with the set $\mathcal{L} = \{\ell(e), e \in E\}$.

B. SPINE DESIGN

The problem addressed at this stage is to find an appropriate spine, which in our case is a spanning tree, i.e., a set of $|V| - 1$ edges connecting all nodes such that a pre-defined minimal target availability $\widehat{a_{WP}}$ for each WP in the spine is achieved at the minimal availability upgrade cost. Alternatively, a pre-defined average target availability for the WPs in the spine, $\widetilde{a_{WP}}$, may also be envisaged.

The availability of the edges of the spine may change (it may be upgraded or downgraded) so that the desired target availability is accomplished. An upgrade of the availability of the edges may be accomplished by having, for instance, a more reliable equipment, backup elements, efficient repair teams that may intervene quickly, if necessary. If a downgrade of the availability of the edges is deemed acceptable, it may be accomplished by allowing an increase of its time to repair by diverting resources into other edges (i.e., by changing the location of spare parts or the efficiency of teams) [70].

Let $a(e)$ represent the final availability of edge e, which may be equal to the initial value $a_0(e)$ or to one of K different pre-defined possible values a_k, $k = 1, \ldots, K$. The cost associated with such a change is calculated as proposed in [70]: $\mathcal{C}(e) = -\ln\left(\frac{1-a(e)}{1-a_0(e)}\right)\ell(e)$. This is a simplified model for the availability upgrade/downgrade cost, which is appropriate in a steady state situation. An enhanced model could be obtained if distances were modified to incorporate some additional information, for instance concerning the vulnerability of the edges. As an example, if an edge is in a disaster-prone area, its modified length could be the actual distance between nodes multiplied by a factor > 1, which would entail a higher cost to guarantee the desired availability. This possibility was not considered when devising the spine, as the information regarding the vulnerability of the edges will be considered later on in the model (in the failure modeling part), and an extra cost may be calculated to reinforce the resilience of edges in disaster-prone areas. Nevertheless, it is considered that the edges in the spine in disaster-prone areas will have a higher level of resistance to disaster concerning the other edges (e.g., stronger ducts).

The selection of the edges forming the spine and their final availability may be accomplished by solving a mixed-integer linear optimization problem (MILP) as detailed in [70] and briefly described in [7]. Note that the problem in [70] is formulated to guarantee that an edge-disjoint BP exists for all demands, which is not required here. Also note that the approach in [70] accepts the downgrade of the availability of the edges that are not in the spine, which allows for a reduction of the total cost. In our approach, the availability of those edges is not changed.

The solution to the mentioned problem for large networks is difficult to obtain in a reasonable time. Therefore, heuristics were developed to try and find an appropriate solution, as in [71], [72]. Still, these approaches could take a few hours to solve moderate-sized problems. To try and find solutions in a shorter time, even for large problems, we now propose a two-stage approach. It starts by finding a set of possible solutions (spines) in a heuristic way, followed by the resolution of a MILP to calculate the final availability for the edges so that a pre-defined target availability ($\widehat{a_{WP}}$ or $\widetilde{a_{WP}}$) is guaranteed. The spine that allows achieving the target availability at a lower cost is selected.

In the heuristics presented in [71], spanning trees that minimize a centrality cost based on a k-betweenness centrality measure [73] are devised. In that heuristic approach, the focus is on more central edges, as least central edges are avoided. Of all the spines found by the heuristics with an edge-disjoint BP for each WP, the spine with the highest average availability for the WPs or the spine with the highest average availability for the path pairs (WP+BP) is the final solution. No availability upgrade is applied.

In the method developed in [72], at a first stage a heuristic was used to obtain a core of the spine, i.e., a set of more central edges with the edge centrality being given by a harmonic centrality measure [74]. It was followed by a second stage, in which a MILP problem was solved to devise the remaining edges of the spine and the final availability for all the edges in the spine. The final solution is the spine guaranteeing a pre-defined target availability $\widehat{a_{WP}}$ at a lower availability upgrade cost.

In this work, we propose an approach also in two stages: (i) at a first stage, a list of possible spines $\mathcal{S}$ is obtained by the heuristic algorithm described in Section IV-C; (ii) at a second stage, the final availability for all the edges in each spine is calculated and the spine satisfying a specific availability level for the WPs and for which the total availability upgrade cost is minimal is selected as the final solution.

In previous works, the focus was solely on guaranteeing a minimal availability $\widehat{a_{WP}}$ of each WP. Here we also consider the possibility of guaranteeing an average availability value $\widetilde{a_{WP}}$ considering all the WPs in the spine. In this case, it is necessary to remove constraint [70, Eq.(22)] and add constraint $1 - \frac{1}{|\mathcal{F}|} \sum_{(s,t)\in\mathcal{F}} \sum_{(i,j)\in E_d} p_{ij}^{st} \geq \widetilde{a_{WP}}$, where $\mathcal{F}$ is the set of demands. The parameters p_{ij}^{st} are continuous variables representing the unavailability of link $(i, j) \in E_d$, given that it is on the WP for demand $s - t$. They are defined in [70, Eq. (20)], which may be used in this case as the parameters x_{ij}^{st} (representing the edges of the WP for demand $s - t$) are no longer variables (they are known beforehand, as the spine is provided to the MILP).

C. HEURISTIC RESOLUTION APPROACH TO DEVISE A LIST OF POSSIBLE SPINES

The heuristics proposed here is based on heuristics presented in [71], [72]. We present the heuristics for devising a list of possible spines $\mathcal{S}$ that will afterwards be considered in a MILP aiming at guaranteeing a minimal availability $\widehat{a_{WP}}$ or an average availability $\widetilde{a_{WP}}$ at minimal availability upgrade cost.

In [72], a study was performed that showed that the trees of a lower diameter length or a lower average length of the WPs could be in some cases associated with the least cost solutions in the final stage of availability upgrade of the edges. We will consider this aspect in the heuristics, as the final list of spines $\mathcal{S}$ will include those with a lower average length of the WPs. Two important features of this heuristic are: (i) all spines are acceptable, even those with unprotected WPs, i.e., with demands for which no pair of edge-disjoint paths exists – this is possible because the GDP-R will still be able to handle these situations; (ii) throughout the heuristics, the spines with a lower average length of the WPs are added to a list of maximum size determined in advance. Therefore (unlike what happened at the heuristics in [71], [72]) the output of this heuristic is a list of spines of a lower average length of the WPs, which will then be provided to a MILP for calculation of the final availability of the edges so that a target minimal availability $\widehat{a_{WP}}$ or average availability $\widetilde{a_{WP}}$ is achieved at minimal availability upgrade cost.

The heuristics is as described in Algorithm 1 (LAL-WP-H). In this heuristic several strategies are used to achieve a diversification of the obtained spines: (i) an edge may be avoided (Lines 22, 36) for a random number of iterations (Lines 21, 35), due to two different criteria; (ii) edges appearing more often in the spines are more penalized (due to cost $\mathcal{C}_{\text{Prim}}(e)$ – see Eq. (1) – used in Line 29); (iii) spines with unprotected paths are acceptable. A detailed description of the heuristic follows.

In the outer `for` cycle, different seeds are considered for the generation of random values. Function `randVal`(*cSeed*, *maxIter*) returns a random value (from a uniform distribution considering a seed *cSeed*), in the set $\{1, 2, \cdots, maxIter\}$.

In the next `for` cycle, a variable *listReset* is either 0 or 1 to indicate whether a list of edges to be avoided when devising possible spines should be reset. This list of edges is one of the strategies used to achieve a diversification of the obtained spines in this heuristic. Therefore, at the inner loop, when *listReset* is 1, then the current list of edges to be avoided is reset (Line 13); otherwise the edges already in the list will continue to be avoided for a number of iterations in *iterAvoid*(·). The inner loop is run a total of $|E| + 1$ times: the first time (*firstTime* is true), no new edge is added to the list of edges to be avoided; the other times (*firstTime* is false), one new edge is added to that list in Line 21, according to a criterion explained next.

Algorithm 1 Heuristic for Devising a List of Spines With a Lower Average Length of the WPs (LAL-WP-H)

Input: $G(V, E)$, $\mathcal{L}$, *maxIter*, *totalSeeds*, *maxSpines*
Output: $\mathcal{S}$

1: Calculate $c_H(e), \forall e \in E$ {Eq. (3)}
2: $initCC(e) \leftarrow \mathcal{C}(e), \forall e \in E$ {Eq. (2)}
3: $maxCC \leftarrow veryHighValue$
4: $iterAvoid(e) \leftarrow 0, \forall e \in E$
5: $initL(e) \leftarrow \ell(e), \forall e \in E$
6: $\mathcal{S} \leftarrow \emptyset$
7: **for** $seed \leftarrow 1$ **to** $totalSeeds$ **do**
8:     $cSeed \leftarrow seed$
9:     **for** $listReset \leftarrow 0$ **to** 1 **do**
10:         $firstTime \leftarrow true$
11:         **loop** $\{|E| + 1$ runs$\}$
12:             **if** $listReset = 1$ **then**
13:                 $iterAvoid(e) \leftarrow 0, \forall e \in E$
14:                 $\ell(e) \leftarrow initL(e), \forall e \in E$
15:             **end if**
16:             **if** $firstTime$ **then**
17:                 $firstTime \leftarrow false$
18:             **else**
19:                 $e' \leftarrow \arg\max_{e \in E: initCC(e) < maxCC} initCC(e)$
20:                 $maxCC \leftarrow initCC(e')$
21:                 $iterAvoid(e') \leftarrow$ `randVal`$(cSeed, maxIter)$
22:                 $\ell(e') \leftarrow veryHighValue$
23:                 Increase $cSeed$
24:             **end if**
25:             **repeat**
26:                 Calculate $c_H(e), \forall e \in E$ {Eq. (3)}
27:                 Calculate $\mathcal{C}(e), \forall e \in E$ {Eq. (2)}
28:                 Calculate $\mathcal{C}_{\text{Prim}}(e), \forall e \in E$ {Eq. (1)}
29:                 $spine \leftarrow$ `Prim`$(\mathcal{C}_{\text{Prim}})$
30:                 **if** $spine$ has at least one unprotected path **then**
31:                     Calculate $averageCC(i), \forall i \in V$
32:                     Identify a demand $s - t$ without disjoint BP
33:                     $i \leftarrow \arg\max_{j \in \{s,t\}} averageCC(j)$
34:                     Select an edge (e) passing in node i
35:                     $iterAvoid(e) \leftarrow$ `randVal`$(cSeed, maxIter)$
36:                     $\ell(e) \leftarrow veryHighValue$
37:                     Increase $cSeed$
38:                 **end if**
39:                 **for all** $e \in E$ **do**
40:                     **if** $iterAvoid(e) > 0$ **then**
41:                       Decrease $iterAvoid(e)$
42:                       **if** $iterAvoid(e) = 0$ **then**
43:                         $\ell(e) \leftarrow initL(e)$
44:                     **end if**
45:                 **end if**
46:              **end for**
47:             **if** $|\mathcal{S}| < maxSpines$ **then**
48:                 $\mathcal{S} \leftarrow \mathcal{S} \cup \{spine\}$
49:             **else**
50:                 $\sigma \leftarrow \arg\max_{\rho \in \mathcal{S}}$ `avgL_WP`(ρ)
51:                 **if** `avgL_WP`$(spine) <$ `avgL_WP`(σ) **then**
52:                     $\mathcal{S} \leftarrow \mathcal{S} \setminus \{\sigma\}$
53:                     $\mathcal{S} \leftarrow \mathcal{S} \cup \{spine\}$
54:                 **end if**
55:             **end if**
56:             **until** a spine without unprotected paths is found
57:         **end loop**
58:     **end for**
59: **end for**

Edges may be avoided (i.e., a very high value is considered as their length $\ell(\cdot)$ during *iterAvoid*$(\cdot)$ iterations) according to two different criteria. In Line 19, one edge at a time is selected to be avoided, with the edges being selected in decreasing order of the initial centrality cost saved in *initCC*$(\cdot)$ (i.e., the least central edges, are avoided first). In Line 34, another criterion is explored: one of the edges in the current spine passing in the origin node or destination node of a demand for which no disjoint BP exists is selected to be avoided. In any case, the edge will be avoided for a random number of iterations.

Each spine is obtained by finding a minimum cost spanning tree (Line 29) using Prim's algorithm [75]. The costs of the edges are

$$\mathcal{C}_{\text{Prim}}(e) = (\mathcal{C}(e) + \ln(\#e + 1))\ell(e) \qquad (1)$$

where $\#e$ is the number of times edge e has already appeared in the obtained spines (penalty imposed to edges appearing more often). The edge length $\ell(e)$ is also a term in this cost, aiming at a focus on shorter edges (as the length of the edges is a term also present in the expression for the availability upgrade cost $\mathcal{C}(e)$). As the edges to be avoided are assigned a length $\ell(\cdot)$ with a very high value, this results in a very high cost $\mathcal{C}_{\text{Prim}}(\cdot)$.

The centrality cost (Line 27) is

$$\mathcal{C}(e) = -c_H(e) + \max_{\mathcal{E} \in E} c_H(\mathcal{E}) + 1 \qquad (2)$$

where

$$c_H(e) = c_H(i,j) = \sum_{n \in V \setminus \{i,j\}} \frac{1}{\min\left(\mu(i,n), \mu(j,n)\right)} \qquad (3)$$

is the harmonic centrality [74] for edge $e \equiv (i,j) \in E$. The parameter $\mu(s,t)$ is the length (in km) of the shortest path between nodes $s, t \in V$. This harmonic centrality assigns each edge a value measuring how close the terminal nodes of an edge are to the other nodes, and it is used here because at certain stages in the algorithm execution the graph may become unconnected. In fact, if for a node pair $i - n$ (and $j - n$) no path may be established, then $\min\left(\mu(i,n), \mu(j,n)\right)$ is infinite and the contribution of this term in the summation to calculate $c_H(i,j)$ is 0. Recall that the less central edges will have the highest $\mathcal{C}(\cdot)$ cost and one such edge is selected in Line 19.

The selection of an edge to be avoided in Line 34 is accomplished by identifying demands for which no edge-disjoint BP exists and considering the node associated to that demand with a higher average centrality (i.e., with a lower average centrality cost calculated as the average value of costs $\mathcal{C}(e)$ for edges e leaving or entering the node – Line 31). An edge of the spine passing in that node is avoided during a random number of iterations. This step is based on a similar step in [71] but it was not considered in [72]. Although it is not mandatory to have edge-disjoint BPs in our resolution approach, it is appropriate to identify the demands with less robust connections.

Note that instead of getting the list of spines $\mathcal{S}$ with a lower average length of the WPs (function `avgL_WP(·)` in Lines 50 and 51), it is possible to obtain a list of spines with other features. It suffices to change the calculated parameter in Lines 50 and 51 of the algorithm and compare the appropriate parameter value in Line 51 for addition of the spines to the list. In particular, instead of getting the list of spines with a lower average length of the WPs, other parameters, such as a lower diameter length (maximal length of any path in the spine) or a lower total length (sum of lengths of all the edges in the spine), were also considered, but the results were the same or worse (in terms of availability upgrade cost) than those obtained when the average length of the WPs was considered.

D. COMPLEXITY ANALYSIS OF THE SPINE COMPUTATION

Let $|V|$ and $|E|$ denote the number of nodes and edges in G, respectively. The time complexity of the heuristic algorithm (Algorithm 1) is determined by the length of the cycles and the operations within, namely the complexity of the Prim's algorithm. In our implementation, the complexity of the Prim algorithm is $O(|V|^2)$, as the graph was represented using an adjacency matrix.

The complexity of the initial steps in Lines 1-6 is $O(|E|)$. The remaining of the algorithm has complexity: $O(totalSeeds \times |E| \times (|E| + \varrho \times |V|^2))$, where ϱ is the number of iterations of the `repeat` cycle (Lines 25-56). In `repeat` cycle there are operations proportional to $|E|$ and *maxSpines*, but as $|V|^2$ is at least an order of magnitude greater than those terms they were suppressed. Therefore, we can estimate the time complexity of the heuristic algorithm to be $O(totalSeeds \times |E| \times \varrho \times |V|^2))$.

The value of ϱ is highly dependent on the number of spines with protected WPs that may be found in each network. In more meshed networks, it is easier to devise spines for which disjoint BPs may be found for each demand, and the number of runs of the `repeat` cycle will be low; for sparser networks, the value of ϱ will be higher and we have limited it to 5000 (which is omitted in the pseudo-code for simplicity).

As for the MILP, recall that it takes each spine of the list of spines $\mathcal{S}$ and calculates the assignment of availability values to each of the edges of the spine, so that a target availability is guaranteed at minimal cost. To illustrate the size of the MILP next, we enumerate the number of variables and constraints. Considering the notation in [70], the variables to consider are r_{ij}^k (binary variables that indicate whether the k-th value of availability is selected for link $(i,j) \in E_d$), and p_{ij}^{st} (already explained in Section IV-B). Therefore, the maximum number of variables is $2(|V| - 1) \times ((K + 1) + |\mathcal{F}|)$, where $K + 1$ is the total number of possible availability values and $|\mathcal{F}|$ is the number of demands. The number of constraints is $2(|V|-1) \times (1+|\mathcal{F}|)+|\mathcal{F}|$, with the first term corresponding to [70, Eqs. (18)-(20)], and the last term corresponding to [70, Eq. (22)] (this term is 1 if the expression for $\widetilde{a_{WP}}$ is used instead, as explained in Section IV-B).

V. FAILURE MODELING PHASE

The task of failure modeling is to transform complex real-world data (network specifications, disaster forecasts, etc.) into a simple form to ensure inputs for survivable routing, network planning, and so on. For the upgrade method presented in the next section, the failure modeling module answers the following question: *Which are those link sets that fail with a strictly positive probability during the next disaster, and what are their probabilities?* The answer can be given in the form of a list of Probabilistic Shared Risk Link Groups (PSRLGs) that is, by definition, a list of link sets, each with a related (failure) probability.[3]

A. GENERAL FRAMEWORK ON FAILURE MODELING

From among the myriad possible PSRLG definitions, we chose a standard definition proposed by [76] that meets our needs and goes as follows. For a link set $S \subseteq E$, the **Cumulative Failure Probability** of S (denoted by CFP(S)) is the probability that *at least S* will fail (and possibly other links too). We will call link sets S with CFP(S) > 0 as PSRLGs, or, if their exact cumulative failure probability is not important, simply as SRLGs. Sometimes we will refer as CFP to CFP(S) of a link set S. For a graph G, we will denote the collection of PSRLGs by CFP[G] (since we store the CFPs alongside the link sets).

Computing a realistic list CFP[G] is not an easy task though, since it needs a deep understanding of the nature of the possibly occurring disasters, topped with a realistic failure model. In this paper, we apply the model described in [16], as follows. We suppose there is at most one disaster in the investigated time period, and we calculate the PSRLGs of the next occurring disaster. The next disaster is treated as a random variable having an epicenter and size. Our other assumption is that those network elements, which intersect the disaster region, fail. This way, we may slightly overestimate the failure probabilities of the link sets, but this issue is inferior to the defects of other models that implicitly assume that links fail independently of each other [77]–[79], and/or use hazard heat maps instead of disaster scenarios [78]. These approaches result in serious under-estimations of the CFP values, making telecom providers to miss certain availability requirements (e.g., five-nine availability).

To be precise, we slightly generalize the disaster regions to be smaller for a more reliable network equipment, and larger for less reliable ones. Therefore, an upgrade of the equipment translates to lower CFP values. Contrary to prior frameworks [7], [14] that are based on the steady state availability of the links as a measure of their disaster intensity tolerance, this model relies on the *real* tolerance of the links to different kinds of disasters. These intensity tolerances are given as part of the input and can be computed by experts (seismologists, climatologists, etc.).

B. ASSESSING THE DISASTER HAZARD

The previously outlined failure model is general. Moreover, it may jointly deal with multiple disaster types [16]. However, in the current work, to save space, we refrain from repeating it in its general form. Instead, we focus on a concise description of its version applied to modeling only the seismic hazard. We chose modeling the threat caused by the earthquakes because the best pre-processing methods for PSRLG computation are available for this disaster family [80].

To model regional failures caused by an earthquake in the case of network equipment having different shaking intensity tolerance, we sightly generalize the model from [80], which combines a discrete version of the previously described failure model with well-founded seismological considerations. In this setting, we are investigating the failures caused by the next earthquake.

The earthquake is identified with its epicenter and moment magnitude: **epicenter** $c_{i,j}$, which represents a latitude-longitude cell on the Earth's surface, taken from a grid of cells over the network area; **moment magnitude** $M_w \in \{4.6, 4.7, \dots\} =: \mathcal{M}$. We index the cell grid such that $i \in \{1, \dots, i_{max}\} =: \mathcal{I}_i, j \in \{1, \dots, j_{max}\} =: \mathcal{I}_j$.

Let $\mathcal{E}_{i,j,M_w}$ denote the set of earthquakes with center point in $c_{i,j}$ and magnitude in $(M_w - 0.1, M_w]$. We will represent all $\mathcal{E}_{i,j,M_w}$ by a single earthquake having a center point in the center of $c_{i,j}$ and a magnitude of M_w. As earthquakes can occur anywhere in the cell, to avoid underestimating the destruction caused by any of the represented earthquakes, we increase the disaster radius of $\mathcal{E}_{i,j,M_w}$ by the distance between the center of the cell and its outer corners (which is considered to be small). Let the probability that the next earthquake is in $\mathcal{E}_{i,j,M_w}$ be p_{i,j,M_w}.[4]

Each network link $e \in E$ can withstand seismic shocks of a given intensity $H(e)$, meaning if an earthquake hits e somewhere with an intensity higher than $H(e)$, the link will fail; otherwise, it will remain intact. We will call $H(e)$ the *intensity tolerance* of link e. We apply the intensity prediction equation of [84] and [85], for Europe, and the USA, respectively. Note that [84] predicted intensities for Italy, and, in this paper, it is used as a first approximation for Europe because of the apparent absence of such a prediction for Europe. According to [84] and [85], the expected intensity I at a site located at epicentral distance R is:

$$I_{\text{It,EU}} = 1.621M_w - 1.343 - 0.0086(D - h)$$
$$- 1.037(\ln D - \ln h) \quad (4)$$
$$I_{\text{US}} = 0.44 + 1.70M_w - 0.0048D - 2.73\log_{10} D \quad (5)$$

where $D = \sqrt{R^2 + h^2}$ is a sort of hypocentral distance, and h represents the hypocentral depth, which may be viewed as the average depth of the apparent radiating source [84], h

---

[3]Note that in the viewpoint of connectivity, the failure of a node can be modeled with the failure of the links incident to it.

[4]In [80], a mature way of determining these probabilities based on historical earthquake catalogs is described. In this work, we evaluated the model of [80] for Italy and the USA from the most recent published earthquakes catalogs ([81] and [82], for Italy and the USA, respectively) that cover long periods of time. For European networks outside of Italy, we used the pre-existing data base [83].
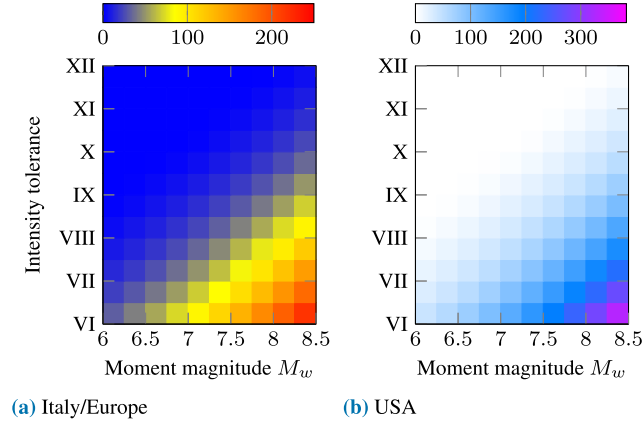
(a) Italy/Europe   **(b)** USA

FIGURE 5. Disaster radii $R(M_W, H)$ (in km) in function of moment magnitude and intensity tolerance according to Eqs. (4) and (5), for Italy and the USA, respectively; the strongest considered earthquake for Italy and the USA is of $M_W = 8.1$ and 8.4, respectively.

equaling 3.91 km and 10 km for Italy/Europe and the USA, respectively. These two particular regions are considered, since the networks used in our study (Section VII) are backbone topology networks of (parts of) Europe and the USA.

After each earthquake $\mathcal{E}_{i,j,M_w}$, the physical infrastructure (such as optical fibers, amplifiers, routers, and switches) with intensity tolerance H in an area $disk(c_{i,j}, R(M_w, H))$ of a circular disk is destroyed. The center point of $disk(c_{i,j}, R(M_w, H))$ is the center of $c_{i,j}$, while its radius $R(M_w, H)$ is monotone increasing in magnitude M_w, and decreasing in H, as depicted in Fig. 5. Note that the intensities are calculated differently for Italy/Europe and the USA. In the case of an intensity tolerance $H = $ VI, the disaster radius $R(M_w, H)$ is still 0 km for earthquakes as strong as $M_w = 4.5$ for Italy/Europe, and $M_w = 4.9$ for the USA, and reaches a maximum of ~ 200 km for the strongest considered earthquake scenario in Italy with $M_w = 8.1$, and ~ 360 km in the worst scenario of the USA with a magnitude of $M_w = 8.4$ (that are the two regions studied in detail in the simulations). For $H = $ X, these worst-case radii are 19 km and 43 km for Italy and the USA, respectively. Note again that we increase the radius (if being strictly positive) by the distance between the center of the cell and its outer corners.

We assume an earthquake $\mathcal{E}_{i,j,M_w}$ destroys every link of network G with intensity tolerance H that has a point in $disk(c_{i,j}, R(M_w, H))$. Let us denote the set of failed links by F_{i,j,M_w}. Let $I_{i,j,M_w}(S)$ be the indicator variable of earthquake $\mathcal{E}_{i,j,M_w}$ hitting at least link set S. This way:

$$I_{i,j,M_w}(S) = \begin{cases} 1, & \text{if } F_{i,j,M_w} \supseteq S \\ 0, & \text{otherwise} \end{cases} \qquad (6)$$

Note that $I_{i,j,M_w}(S)$ also depends on the intensity tolerances $H(e)$ of the links of set S. For a link set S, CFP(S) can be calculated as:

$$\text{CFP}(S) = \sum_{i,j \in \mathcal{I}_i \times \mathcal{I}_j} \sum_{M_w \in \mathcal{M}} p_{i,j,M_w} I_{i,j,M_w}(S) \qquad (7)$$

We note that [76] also offers a more compact representation of the disaster hazard that can be useful if the storage size of CFP[G] exceeds the available memory space.

VI. DISASTER-RESILIENT NETWORK PLANNING

Due to the failure modeling, the PSRLGs show a realistic picture of the network's possible failures in the case of a disaster. Some of these potential failures disconnect the network, disrupting the communications. If the network remains connected after the given disasters, i.e., after each failure in the SRLG list, then the GDP-R can protect the connection against all of them. This problem can be controlled with the introduction of the disconnection probability threshold (T_D), which is the target probability of our novel upgrade methods.

Our goal is to ensure that the probability of the network to fall apart after a disaster is less than T_D, i.e., the summed probability of the earthquakes causing a network disconnection (P_D) has to be lower than T_D.

Since we aim to ensure the connectivity of the network with the lowest intensity tolerance upgrade cost possible, an ILP is proposed in this paper to find the optimal upgrade level for each link. To reduce resource consumption and running time, two heuristic methods are introduced and compared to the ILP from the intensity tolerance upgrade cost and computation time point of view.

The intensity tolerance upgrade cost used by the earthquake resilience upgrade methods is directly proportional to the length of the link. In this regard, it is similar to the availability upgrade cost used by the spine. Note that the earthquake resilience upgrade cost is independent from the initial intensity tolerance of the link. Other than the length of the link, it is only related to the volume of the upgrade (as expressed by the objective function in Eq. (8)). For example, upgrading a link from level VI to level VII (one-level upgrade) costs half as much as upgrading it from level VI to level VIII (two-level upgrade). Therefore, *the two upgrade costs, i.e., the availability upgrade cost and the intensity tolerance upgrade cost, are not summable or even comparable.* These costs refer to the upgrade of different features of the edges in this framework for disaster resilience: availability (associated with a steady state of the network) and tolerance to withstand disasters, in particular earthquakes.

We consider that every network link $e \in E$ has an initial intensity tolerance $H_0(e)$, which can be increased by $\Delta H(e)$ to a higher level ($H(e) = H_0(e) + \Delta H(e)$) at cost $\Delta H(e) * \ell(e)$, where $\ell(e)$ is the length of the link. $\mathbf{H_0}$ denotes the vector of the initial intensity tolerances ($H_0(e)$) for every network link $e \in E$. Similarly $\Delta \mathbf{H}$ and $\mathbf{H}$ represent the vector of the upgrade levels and the final intensity tolerances, such that $\mathbf{H} = \mathbf{H_0} + \Delta \mathbf{H}$.

To determine if link $e \in E$ with intensity tolerance $H(e)$ fails in the case of an earthquake at $p \in \mathcal{P}$ with magnitude $M_w \in \mathcal{M}$, the earthquake's intensity has to be known at the link. It is denoted by $I(e, p, M_w)$ and calculated according to Eq. (4) in the case of Italy and according to Eq. (5) in the case of the USA. The matrix of the $I(e, p, M_w)$ values is denoted

TABLE 3. Notation used in Section VI.

Notation	Description
$G(V, E)$	Input graph, its node set and edge set, respectively
$\mathcal{N}$	Set of minimum cuts
S	Set of links in a minimum cut
$\mathcal{P}$	Set of grid points
$\mathcal{M}$	Set of earthquake magnitudes
$Pr(p, M_w)$	Probability of an earthquake at point $p \in \mathcal{P}$ with magnitude $M_w \in \mathcal{M}$
P_D	Probability that the network will fall apart because of the next earthquake
T_D	Probability threshold, which specifies the scope of the defense. The goal is to decrease the probability of falling apart below this threshold.
$I(e, p, M_w)$	Intensity of an earthquake with epicenter p and magnitude M_w at link e
$H(e)$	Intensity tolerance of link e: $H(e) = H_0(e) + \Delta H(e)$
$H_0(e)$	Initial intensity tolerance of link e, integer
$\Delta H(e)$	Intensity tolerance upgrade for link e, integer
$y(e, p, M_w)$	Binary variable for failure of link e in the case of an earthquake centered at p with magnitude M_w: 1 if it fails, else 0.
$z(S, p, M_w)$	Binary variable for failure of set S in the case of an earthquake centered at p with magnitude M_w: 1 if all links of S fail, else 0.
$w(p, M_w)$	Binary variable for earthquake with epicenter p and magnitude M_w: 1 if it disconnects the network, else 0.
$\ell(e)$	Length of link e

with $\mathbf{I}$. The probability of the given earthquake is denoted as $Pr(p, M_w)$, while the matrix of the probability values is denoted as $\mathbf{Pr}$. The notations used in this section are defined in Table 3.

A. INTEGER LINEAR PROGRAM FOR LINK UPGRADE

To ensure the connectivity of the network with a certain probability level for the minimal total intensity tolerance upgrade cost, an ILP was implemented.

The ILP has four different variables:

(a) $y(e, p, M_w)$ is a binary variable, which indicates if link e fails in the case of an earthquake at p with magnitude M_w;

(b) $z(S, p, M_w)$ is a binary variable, which indicates if link group S fails ($y(e, p, M_w) = 1$, $\forall e \in S$) in the case of an earthquake at p with magnitude M_w;

(c) $w(p, M_w)$ is a binary variable, which indicates if an earthquake at p with magnitude M_w disconnects the network;

(d) $\Delta H(e)$ is an integer variable, it is the intensity tolerance upgrade for link e.

The ILP contains three sets of constraints, Eqs. (9)-(11), and a final constraint, Eq. (12). The first set of constraints (Eq. (9)) implies that if the intensity of an earthquake at link e is higher than the intensity tolerance of the link ($H(e)$) then the link fails. The second set (Eq. (10)) grants that link group S fails if every link in link group S fails. The third set of constraints (Eq. (11)) assures that if an earthquake

hits a minimal cut, then it disconnects the network. Finally, Eq. (12) is a constraint, which forces the probability of falling apart to be lower than T_D. As we emphasized before, our goal is to minimize the total intensity tolerance upgrade cost of the network, which is reflected in the objective function (Eq. (8)). The ILP is formalized as follows:

$$\min \sum_{e \in E} \ell(e) \cdot \Delta H(e) \tag{8}$$

$$\text{subject to}: y(e, p, M_w) \geq 1 - \frac{H_0(e) + \Delta H(e)}{I(e, p, M_w)}$$
$$\forall e \in E, p \in \mathcal{P}, M_w \in \mathcal{M} \tag{9}$$

$$z(S, p, M_w) \geq \sum_{e \in S} y(e, p, M_w) - |S| + 1,$$
$$\forall S \in \mathcal{N}, \quad p \in \mathcal{P}, M_w \in \mathcal{M} \tag{10}$$

$$w(p, M_w) \geq z(S, p, M_w), \quad \forall S \in \mathcal{N},$$
$$p \in \mathcal{P}, M_w \in \mathcal{M} \tag{11}$$

$$\sum_{\substack{p \in \mathcal{P} \\ M_w \in \mathcal{M}}} Pr(p, M_w) \cdot w(p, M_w) \leq T_D \tag{12}$$

$$\Delta H(e) \text{ integer}, \quad \forall e \in E \tag{13}$$

$$y(e, p, M_w), \quad z(S, p, M_w) \text{ binary},$$
$$\forall e \in E, S \in \mathcal{N}, p \in \mathcal{P}, M_w \in \mathcal{M} \tag{14}$$

$$w(p, M_w) \text{ binary}, \quad \forall p \in \mathcal{P}, M_w \in \mathcal{M} \tag{15}$$

As explained earlier, $I(e, p, M_w)$ (in Eq. (9)) is the intensity of an earthquake with epicenter p and magnitude M_w at link e. The intensity is calculated according to Eq. (4) in Italy and according to Eq. (5) in the USA.

Note that Eqs. (10)-(11) could be merged into one single set of constraints and then variables $z(S, p, M_w)$ would not be necessary. However, for clarity, we have left the formulation in its current form.

This ILP may not be scalable for large networks and SRLG lists, so we devised heuristic algorithms for solving the decrease of the disconnection probability in a suboptimal way.

B. LINK UPGRADE HEURISTIC METHOD BASED ON THE OCCURRENCES IN CUT SRLGs (Baseline HEURISTIC – BH)

Algorithm 2 presents our simplest solution, which serves as a baseline and demonstrates that a more complex method is needed to approach the optimal solution. The iterative process upgrades one link with one level at every step until the disconnection probability of the network (P_D) is lower than the predefined threshold T_D.

At each step, the links of G are ranked based on their occurrences in the minimal-cut SRLGs in $\mathcal{N}$. The occurrence counts are kept in vector E^* and the link with the highest occurrence count is selected for an upgrade. If multiple links share the same (highest) occurrence count then the one with the lowest intensity tolerance upgrade cost (i.e., with the lowest length) is selected for an upgrade. After upgrading the intensity tolerance of the selected link with one level, the disconnection probability is recalculated using the

Algorithm 2 A Baseline Heuristic Algorithm (BH) to Calculate a Possible Intensity Tolerance Upgrade for Network G Based on the Occurrences in Cut SRLGs, to Decrease the Probability P_D of Falling Apart Below the Probability Threshold T_D

Input: $G(V, E)$, $\mathcal{L}$, $\mathbf{H_0}$, $\mathbf{I}$, $\mathbf{Pr}$, $\mathcal{N}$, P_D, T_D
Output: $G(V, E)$, $\mathbf{H}$: graph with improved earthquake resilience

---

1: $\mathbf{H} \leftarrow \mathbf{H_0}$ {Initial intensity tolerance}
2: **while** $P_D > T_D$ **do**
3:   $E^*(e) \leftarrow 0, \forall e \in E$
4:   **for all** $S \in \mathcal{N}$ **do**
5:    **for all** $e \in S$ **do**
6:     $E^*(e) \mathrel{+}= 1$
7:    **end for**
8:   **end for**
9:   $e_u \leftarrow e_1$ {First link in G}
10: **for all** $e \in E$ **do**
11:   **if** $E^*(e) = \max_{\varepsilon \in E}(E^*(\varepsilon))$ **then**
12:    **if** $\ell(e) < \ell(e_u)$ **then**
13:     $e_u \leftarrow e$
14:    **end if**
15:   **end if**
16: **end for**
17: $H(e_u) \mathrel{+}= 1$
18: $P_D \leftarrow \mathtt{calcFAprobability}(G, \mathcal{N}, \mathbf{I}, \mathbf{Pr}, \mathbf{H})$
19: **end while**

`calcFAprobability` function and the upgrade continues until $P_D < T_D$ (the network's probability of falling apart is less than the threshold).

C. LINK UPGRADE HEURISTIC METHOD BASED ON THE DISCONNECTION PROBABILITY (DPH)

Our other heuristic algorithm (Algorithm 3) is also an iterative method, which upgrades one link with one level at every step, but it utilizes a different approach to select the next link to upgrade. Differently from Algorithm 2, where at each step the next link for an upgrade is selected based on the occurrence count in the minimal-cut SRLGs, in Algorithm 3 the decision is based on the probability decrease of P_D (the network's probability to fall apart) that the link's upgrade would entail, and the intensity tolerance upgrade cost of the link together.

At each step, we investigate by how much the disconnection probability will decrease in the case of a link upgrade. The disconnection probability in the case of the upgrade of link e is $P'_{D,e}$. Since we are only interested in decreasing the probability below T_D, the probability decrease for link e is $P_D - \max\left(P'_{D,e}, T_D\right)$. To find the highest probability decrease for a unit cost, the total probability decrease of a link is divided by the one-level intensity tolerance upgrade

cost of the link.

$$P_{\eta,e} = \frac{1}{\ell(e)} \left(P_D - \max\left(P'_{D,e}, T_D\right)\right) \qquad (16)$$

At each step, the link with the highest probability decrease for a unit cost is selected for an upgrade. After each upgrade step, the disconnection probability (P_D) is recalculated. The upgrade process ends when the probability that the network will fall apart reaches the probability threshold (T_D).

Algorithm 3 A Disconnection-Probability-Based Heuristic Algorithm (DPH) to Calculate a Possible Intensity Tolerance Upgrade for Network G Based on Disconnection Probabilities, to Decrease the Probability P_D of Falling Apart Below the Probability Threshold T_D

Input: $G(V, E)$, $\mathcal{L}$, $\mathbf{H_0}$, $\mathbf{I}$, $\mathbf{Pr}$, $\mathcal{N}$, P_D, T_D
Output: $G(V, E)$, $\mathbf{H}$: graph with improved earthquake resilience

---

1: $\mathbf{H} \leftarrow \mathbf{H_0}$ {Initial intensity tolerance}
2: **while** $P_D > T_D$ **do**
3:   $P_{\eta,max} \leftarrow 0$ {maximum probability decrease steepness}
4:   $e_u \leftarrow e_1$ {First link in G}
5:   **for all** $e \in E$ **do**
6:    $H(e) \mathrel{+}= 1$
7:    $P'_{D,e} \leftarrow \mathtt{calcFAprobability}(G, \mathcal{N}, \mathbf{I}, \mathbf{Pr}, \mathbf{H})$
8:    $P_{\eta,e} = \frac{1}{\ell(e)}(P_D - \max(P'_{D,e}, T_D))$
9:    **if** $P_{\eta,e} > P_{\eta,max}$ **then**
10:    $e_u \leftarrow e$
11:    $P_{\eta,max} \leftarrow P_{\eta,e}$
12:   **end if**
13:   $H(e) \mathrel{-}= 1$
14: **end for**
15: $H(e_u) \mathrel{+}= 1$
16: $P_D \leftarrow \mathtt{calcFAprobability}(G, \mathcal{N}, \mathbf{I}, \mathbf{Pr}, \mathbf{H})$
17: **end while**

D. COMPLEXITY ANALYSIS OF THE DISASTER-RESILIENT NETWORK PLANNING

Let $|\mathcal{N}|$ denote the number of minimal cuts (with an upper bound of $|V|(|V|-1)/2$), $\overline{|S|}$ the average size of the minimal cuts (with an upper bound of $|V| - 1$), $|\mathcal{P}|$ the number of epicenters, $|\mathcal{M}|$ the number of magnitudes, h_{BH} the number of upgrade steps performed by the baseline heuristic algorithm and h_{DPH} the number of upgrade steps performed by the disconnection-probability-based heuristic algorithm.

If a limitation to the number of upgrade levels is considered (omitted in the pseudo-code for simplicity), i.e., there are only $|\mathcal{H}|$ possible different upgrade levels, then the number of upgrade steps has an upper bound of $|E| \times |\mathcal{H}|$.

Since the `calcFAprobability` function has a significant part in both heuristic algorithms, we give its complexity first and then reuse the result later. The time complexity of

calcFAprobability is $O(|\mathcal{N}| \times \overline{|S|} \times |\mathcal{P}| \times |\mathcal{M}|)$, that is $O(|V|^3 \times |\mathcal{P}| \times |\mathcal{M}|)$.

The time complexity of both heuristic algorithms depends on the number of iterations the algorithms have to make to find a solution and the complexity of the iterations. In case of the BH, one iteration consists of 3 parts: (1) the counting of the edges' occurrences in the min-cuts which has a complexity of $O(|\mathcal{N}| \times \overline{|S|})$; (2) selecting the shortest link from the ones with the highest occurrence count which has a complexity of $O(|E|)$; and (3) upgrading the network and recalculating the disconnection probability which has a complexity of $O(|V|^3 \times |\mathcal{P}| \times |\mathcal{M}|)$. With this in mind, the time complexity of BH is $O(|E| \times |V|^3 \times |\mathcal{P}| \times |\mathcal{M}|)$.

In case of the DPH, one iteration consists of 2 parts: (1) the calculation of the steepness of the disconnection probability decrease for each edge which has a complexity of $O(|E| \times |V|^3 \times |\mathcal{P}| \times |\mathcal{M}|)$; and (2) upgrading the network and recalculating the disconnection probability which has a complexity of $O(|V|^3 \times |\mathcal{P}| \times |\mathcal{M}|)$. Note that in both parts the complexity of the calcFAprobability function is reused. Accordingly, the time complexity of DPH is $O(|E|^2 \times |V|^3 \times |\mathcal{P}| \times |\mathcal{M}|)$.

To illustrate the size of the ILP, we enumerate the number of variables and constraints. The variables in our ILP are $\Delta H(e)$, $y(e, p, M_w)$, $z(S, p, M_w)$ and $w(p, M_w)$. The counts of the particular variables are $|E|$, $|E| \times |\mathcal{P}| \times |\mathcal{M}|$, $|\mathcal{N}| \times |\mathcal{P}| \times |\mathcal{M}|$ and $|\mathcal{P}| \times |\mathcal{M}|$, respectively. The number of constraints is almost identical to the number of variables: Eq. (9) creates $|E| \times |\mathcal{P}| \times |\mathcal{M}|$ constraints, Eq. (10) creates $|\mathcal{N}| \times |\mathcal{P}| \times |\mathcal{M}|$ constraints, Eq. (11) creates $|\mathcal{N}| \times |\mathcal{P}| \times |\mathcal{M}|$ constraints and Eq. (12) creates 1 constraint. Additionally, if the possible upgrade levels are bounded it creates $2 \times |E|$ constraints (omitted in the formulation for simplicity). The large number of variables and constraints can lead to extensive resource consumption in terms of memory.

VII. EXPERIMENTAL RESULTS

In this section, we provide a comprehensive study of the different aspects of eFRADIR. Table 4 provides information concerning the network topologies used in the evaluation. The janos-us, cost266 and germany50 network topologies were taken from [86], and the lengths of the links were defined as the distances between nodes assuming that longitude and latitude coordinates are known for each node. As for the Interoute[5] network (a backbone network in Italy [80]), the links were defined as a series of points (starting with the source and ending with the target node) with straight lines between them. In this case, the length of the link is defined as the summed length of the straight lines of the link assuming that longitude and latitude coordinates are known for each point. Since the Interoute network contains a parallel edge pair between the nodes in Sardinia, the longer one was removed for devising the spine. Note that the cost266 and germany50 networks are only used at the runtime and scalability analysis of the

---

[5] https://github.com/mogyi006/eFRADIR

TABLE 4. Network characteristics ($|V|$, $|E|$, γ – average node degree).

Network	$|V|$	$|E|$	γ
janos-us [86]	26	42	3.23
Interoute [80]	25	35	2.72
cost266 [86]	37	57	3.08
germany50 [86]	50	88	3.52

disaster-resilient network planning. The earthquake probability data is obtained from [80] for the Interoute network, and calculated based on earthquake catalog [82] for janos-us. The routing cost $c(e)$ for edge $e \in E$ corresponds to the cost of allocating a unit of demand (i.e., wavelength) on e. Since in this work, we assumed unitary routing costs, the routing cost efficiency was equivalent to the capacity efficiency.

In this section, we first present the results regarding the steady state network planning, i.e., spine in Section VII-A. Next, we analyze the disaster preparedness, in particular, we analyze the probabilities related to SRLGs in Section VII-B and the routing in the non-upgraded network scenario in Section VII-C. In Section VII-D the cost of disaster-resilient network planning is assessed, i.e., the cost comparison of the different upgrade methods is presented. We compare the scenarios with and without the spine. Finally, in Section VII-E, we investigate the survivable routing methods (GDP-R and SRLG Diverse Routing) concerning the average capacity allocated per connection, the average availability of all (non-blocking) connections and the blocking probability in the upgraded scenario.

We would like to emphasize that if the SRLG list does not contain all the links, the Diverse Routing does not necessarily find two edge-disjoint paths. Therefore, the $1 + 1$ SRLG disjoint protection may be considered a particular case of Diverse Routing when all the links are included in the SRLG list. Regarding the average capacity allocation, the joint segments of the paths are calculated as shared resources, hence for the two paths only one unit of capacity is allocated on the given segment (making it more comparable to the GDP-R).

The demands were generated between all $s - t$ pairs with unit bandwidth requirements.

Note that due to the fundamental differences in failure modeling (a novel complex earthquake activity and magnitude-based failure model instead of a ground-shaking hazard model) the experimental results are not comparable to the previous ones presented in [14] and [7]. The input networks, seismic data, and some results are available in our GitHub repository eFRADIR, where a simple example of how eFRADIR works is also provided.

A. RESULTS FOR THE SPINE

In the networks studied, the number of pre-defined possible values for the availability is $K = 4$. For the janos-us network, we considered $a_1 = 0.99$, $a_2 = 0.995$, $a_3 = 0.999$, $a_4 = 0.9995$. For the Interoute network, we considered $a_1 = 0.995$, $a_2 = 0.999$, $a_3 = 0.9995$, $a_4 = 0.9999$.

TABLE 5. Best-cost results (in terms of availability upgrade costs).

Availabilities \\ Networks	janos-us	Interoute
$\widehat{a_{WP}}$ 0.99	12,841.99	
0.992	15,495.99	
0.995	20,709.54	3,095.73
0.997		5,615.07
$\widetilde{a_{WP}}$ 0.995	10,452.27	
0.997	18,747.81	
0.999		6,851.90
0.9992		7,929.63

The best-cost results (in terms of availability upgrade costs) presented in Table 5 were obtained when the heuristics described in Section IV-C was used to get a list of spines that were afterwards provided to the MILP. The maximum value considered for *maxSpines* was 30, while the total number of possible trees for any of the considered networks was, however, substantially higher.

The spines with the best availability upgrade cost for the janos-us network that guarantee $\widehat{a_{WP}} = 0.99$ and $\widehat{a_{WP}} = 0.995$ are displayed in Figs. 6(a)-(b), respectively. The spines are quite similar, as they only differ in a pair of edges. The spines with the best availability upgrade cost (guaranteeing the target availabilities considered in Table 5) for the Interoute network are presented in Figs. 6(c)-(d). The two spines differ in two pairs of edges only. This is in accordance with an aspect observed in [72]: interesting solutions tend to include a set of edges that form the most central part of the spine, and only a few edges change from one good solution to another.

B. ANALYSIS OF PROBABILISTIC SRLGs
As in this subsection, the probabilities related to SRLGs play a central role, we will refer to them as PSRLGs. Figs. 7 and 8 provide information on the number of PSRLGs, and their average size (i.e., the average number of links they contain), for different probability bins, respectively. The intensity tolerance of the links was assumed to be the basic, $H(e) = \text{VI}$, for every $e \in E$. The probability bins were taken as equal intervals on the logarithmic scale.

We can see that for Interoute, both the number and probability of PSRLGs are higher compared to the janos-us topology. It is because the former network has a relatively smaller geographic coverage compared to the earthquake disaster zones. Due to the shorter links, the earthquakes in the area of Interoute can hit a large number of network links at the same time. Therefore, the average size of PSRLGs with probabilities in $[2 \cdot 10^{-8}, 10^{-5}]$ typically exceeds 5, and, for numerous bins, reaches 6. The janos-us topology is more wide-spread, yielding an average PSRLG size rarely exceeding 4.

As the probability related to the bins grows, the average PSRLG size tends to shrink with it. It is simply because smaller link sets are more likely to fail. At the upper end of the probability scale (around 10^{-2} for both topologies), the average PSRLG size decreases to 1. It means that only single links have a probability of about 1% of failing when the next earthquake strikes this region of the network.

Returning to the number of PSRLGs, Interoute has 11,930 PSRLGs compared to the 751 PSRLGs of the janos-us network. Again, Interoute has more link sets that may fail together because of its relatively smaller geographical extension. In the case of Interoute, after a slight growing tendency, the number of PSRLGs in each bin decreases drastically from $\sim 3,000$ to just 7 in the probability interval $[2 \cdot 10^{-6}, 10^{-2}]$. The initial growing tendency might be simply caused by the fact that there are some PSRLGs with small probability but with a large size x, and all their subsets including those many with $\sim x/2$ elements (that still have only a moderate CFP) are present in some of the bins. The decreasing number of PSRLGs is simply because most of the earthquakes have moderate magnitudes (although having a high cumulative hazard of happening). Thus they can hit only single links, links that are close, or incident to the same node. Similar patterns can be seen for the janos-us topology too, although to a lesser extent.

C. ROUTING IN THE NON-UPGRADED NETWORK
To present the advantages of the GDP-R routing method [56] compared to the SRLG Diverse Routing (ILP formulation of SRLG-disjoint scheme [66]), a simulation was performed for the initial networks (i.e., with no upgrade applied).

The routing methods had to provide a solution between all possible node pairs while protecting the routes against various SRLG lists. These SRLG lists were composed from single link failures, adjacent failures and failures caused by earthquakes. The SRLGs causing partitioning of the network were removed from the single link and adjacent failures, hence the network disconnections were only caused by regional failures. The added earthquake failures were controlled with the T_S probability threshold: only SRLGs with a probability higher than T_S were added (i.e., the operator could tune the protection according to the Service Level Agreements). Tables 6 and 7 include values of blocking probability and the numbers of SRLGs for the relevant T_S values. The obtained blocking probability represented the fraction of connections that the routing method was not able to protect against the given SRLG list. Note that whenever the network remained connected, the GDP-R was able to find a solution and no blocking occurred. Therefore, in the case of GDP-R, the blocking probability was directly implied by network disconnections.

As shown in Tables 6 and 7, since the networks were connected for the first few T_S values, the blocking probability of GDP-R was zero in these cases, while for the DR scheme, the blocking occurred for about 30% of the connections in both networks. With the decrease of T_S, the SRLG lists were growing (Tables 6 and 7). They started to include larger SRLGs, which caused disconnections in the networks. Therefore the blocking probability of GDP-R started to rise. However, it stayed steadily below DR's. Hence we can draw our first conclusion that the GDP-R scheme is superior to the
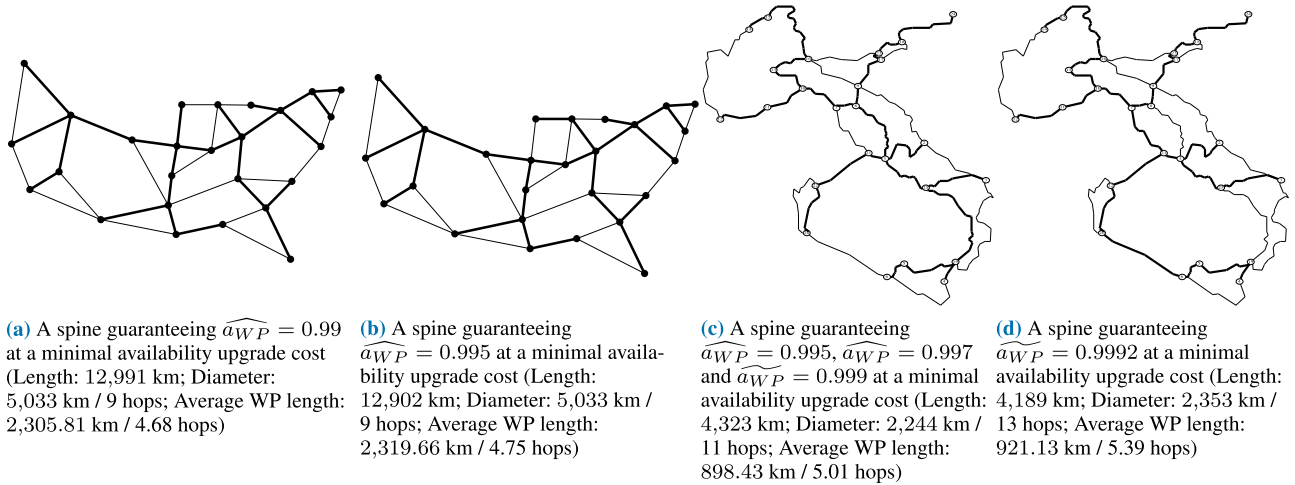
(a) A spine guaranteeing $\widehat{a_{WP}} = 0.99$ at a minimal availability upgrade cost (Length: 12,991 km; Diameter: 5,033 km / 9 hops; Average WP length: 2,305.81 km / 4.68 hops)

(b) A spine guaranteeing $\widehat{a_{WP}} = 0.995$ at a minimal availability upgrade cost (Length: 12,902 km; Diameter: 5,033 km / 9 hops; Average WP length: 2,319.66 km / 4.75 hops)

(c) A spine guaranteeing $\widehat{a_{WP}} = 0.995$, $\widehat{a_{WP}} = 0.997$ and $\widetilde{a_{WP}} = 0.999$ at a minimal availability upgrade cost (Length: 4,323 km; Diameter: 2,244 km / 11 hops; Average WP length: 898.43 km / 5.01 hops)

(d) A spine guaranteeing $\widehat{a_{WP}} = 0.9992$ at a minimal availability upgrade cost (Length: 4,189 km; Diameter: 2,353 km / 13 hops; Average WP length: 921.13 km / 5.39 hops)

FIGURE 6. Spines for the **(a)**, **(b)** janos-us and **(c)**, **(d)** Interoute network.
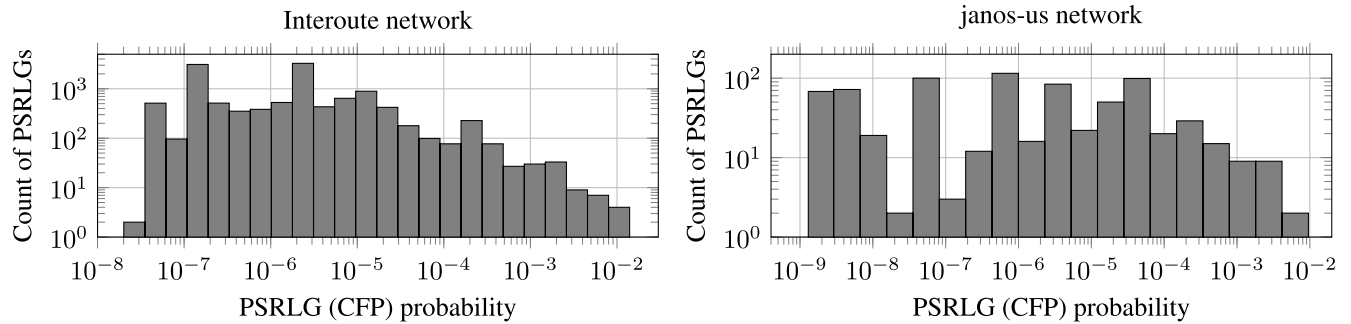

FIGURE 7. Distribution of the PSRLGs based on their probabilities.
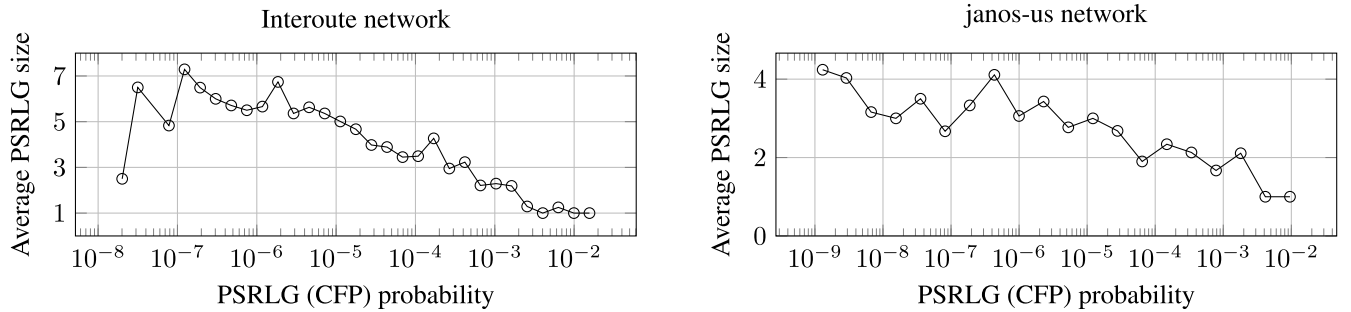

FIGURE 8. The average size of the PSRLGs related to their probabilities.

DR approach in terms of blocking probability (this observation will be further elaborated in the remaining part of this section).

D. RESULTS FOR THE DISASTER-RESILIENT UPGRADE METHODS

The performance of different disaster-resilient upgrade methods was analyzed for the janos-us and the Interoute networks. In both cases, the initial intensity tolerance of all links was set to VI, which meant that the links were expected to fail because of an earthquake if its intensity at the link was higher than VI. The maximal intensity tolerance of a link was IX, i.e., no link survived an earthquake with an intensity higher than IX.

The earthquake rate maps for the two networks were taken from [80]. The maps were discretized by using a sufficiently fine grid over the plane. The Italian rate map had a resolution of 0.02°, while the USA had a resolution of 0.5°. The epicenters where no magnitude had a rate over 0, were discarded. After the preprocessing, the Italian and the USA rate maps contained 3,200 and 3,500 epicenters, respectively. In both maps, the rates between moment magnitudes 4.6 and 8.4 were given, with a resolution of 0.1.

In the initial failure modeling, there were 11,930 SRLGs (333 minimal-cut SRLGs) in the Interoute network and 751 SRLGs (47 minimal-cut SRLGs) in the janos-us network. To rationalize the running time and RAM requirements of the ILP, since the number of minimal-cut SRLGs was too high for

TABLE 6. Values of blocking probability in the non-upgraded Interoute network.

T_S	Block. prob.		Number of
	DR	GDP-R	SRLGs
0.01	0.30	0.0	67
0.005	0.30	0.0	68
0.0025	0.37	0.08	71
0.0016	0.50	0.23	89
0.00155	0.50	0.30	98
0.00125	0.66	0.43	102
0.0011	0.71	0.49	114
0.00065	0.86	0.70	131
0.0004	0.94	0.88	187
0.0003	0.96	0.93	222
0.0002	0.99	0.99	286

TABLE 7. Values of blocking probability in the non-upgraded janos-us network.

T_S	Block. prob.		Number of
	DR	GDP-R	SRLGs
0.01	0.28	0.0	93
0.0075	0.28	0.0	93
0.005	0.28	0.0	93
0.0025	0.28	0.0	96
0.00205	0.34	0.15	101
0.0008	0.46	0.29	106
0.0004	0.464	0.29	111
0.00035	0.52	0.35	117
0.00015	0.52	0.35	135
0.00005	0.63	0.47	160

the ILP, we discarded the least probable minimal-cut SRLGs in the case of the Interoute network, with the probability threshold being as low as 0.00018. Initially, the probability of disconnection (P_D) was 0.02236 in the case of the 333 minimal-cut SRLGs. After keeping only the most probable 45 minimal-cut SRLGs, P_D decreased to 0.022135 (i.e., by only 1%). Note that this preprocessing was not necessary for the heuristics. However, we ran them on the same 45 most probable disaster scenarios to keep the comparisons fair.

The cost efficiency of the three intensity tolerance upgrade methods (two heuristic methods and the ILP) were compared through several T_D values from the [0.0005, 0.01] range. Each method started from the same initial state and it had to provide an upgraded network with $P_D < T_D$. The algorithms were compared based on the intensity tolerance upgrade cost of the solutions and their runtime value.

The effect of the spine was taken into account in the second simulation, where it was assumed that the upgraded availability of the links in the spine corresponded to guaranteeing that those links have an initial intensity tolerance of VII. In this simulation, the upgraded networks providing a minimal target availability $\widehat{a_{WP}} = 0.995$ were used. Apart from the change of the initial intensity tolerance values, the network remained the same.

The algorithms were implemented in Python 3.7.7 on a virtual machine with 8 CPU cores (2.4 GHz) and 32GB of RAM. To create and solve the ILP, the python-mip package (version 1.12.0) was used alongside the Gurobi solver [87] (version 9.0).

The intensity tolerance upgrade costs as a function of different T_D levels are shown in Figs. 9 and 10. In each figure, its left part shows the case where the spine was not considered (i.e., there was no initial modification of the availability of the links). The respective right parts of Figs. 9 and 10, in turn, present results for the devised spine with its links having an initial intensity tolerance of VII. In the case of the Interoute network, the probability of disconnection (P_D) was 0.022360, when every intensity tolerance $H_0(e)$ value was VI. After increasing the $H_0(e)$ values by one for the links on the spine, the probability of disconnection dropped to 0.005859. In the case of the janos-us network, these values were 0.0041 and 0.00172, respectively.

It is clear that in terms of the cost efficiency of intensity tolerance upgrade, the DPH method and the optimal ILP solution outperform the BH method by a large margin in every scenario. This gap becomes much smaller between the two more advanced methods. In the cases where every link had an initial intensity tolerance of VI, the average difference between the intensity tolerance upgrade costs was 2.8%, of course in favor of the optimal ILP solution. On the contrary, when the links on the spine had an initial intensity tolerance of VII, the average gap increased to 8%. Based on that, a conclusion can be drawn that the intensity tolerance upgrade cost for the DPH method is about 5% higher, on average, than the optimal one.

To sum up, we can state that DPH performs very well. Concerning the cost efficiency of intensity tolerance upgrade, it provides results within 5% of the optimal ones (i.e., returned by the ILP), on average. The running time and scalability of the methods is analysed in detail in Section VII-F.

E. ANALYSIS OF THE ROUTING SIMULATIONS FOR THE UPGRADED NETWORK SCENARIO

1) THE EFFECT OF A SPINE ON AVAILABILITY
In Table 8, we compare the average availability of the two routing methods (GDP-R [56] and ILP formulation of SRLG Diverse Routing [66]) at different upgrade levels (expressed by different values of the threshold T_D for the disconnection probability) and minimal SRLG probability thresholds (T_S). Note that the average availability of a given routing method is defined as the average of the connection-wise end-to-end availability calculated with the pivotal decomposition [88] of the sub-graph induced by the routes selected by the routing method.

In the left part of Table 8 (denoted as ''without the spine''), the initial availability values ($a_0(e)$) are used. In the right part (denoted as ''with the spine''), the availability values are upgraded according to the method described in Section IV to guarantee a minimal target availability $\widehat{a_{WP}} = 0.995$. Note that the WPs obtained by the routing methods are not necessarily composed of edges in the spine, hence their minimal availability may not be 0.995.

The used disaster-resilient upgrade solution at every T_D level is the optimal (i.e., the most cost-efficient in terms of
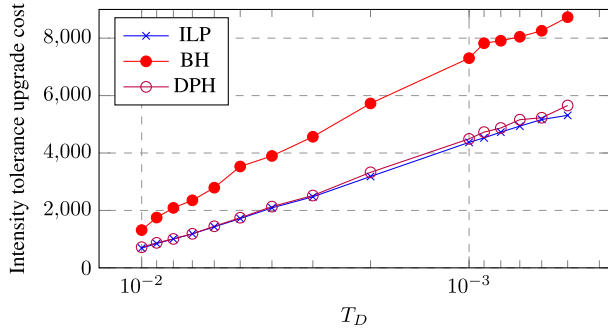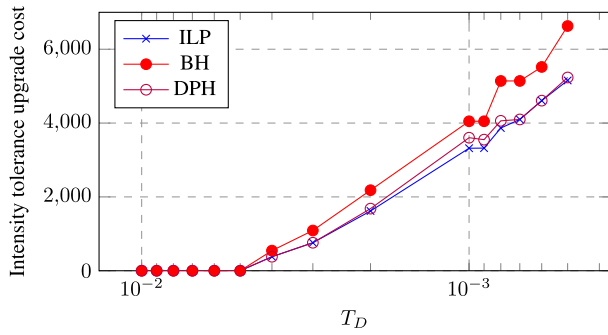
(a) without availability upgrade (i.e., without the spine)
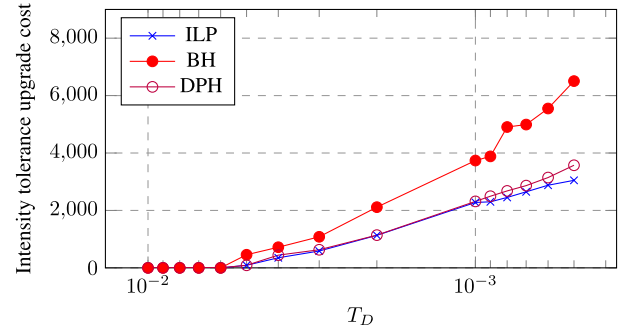
(b) with availability upgrade (i.e., with the spine)

FIGURE 9. Comparison of the intensity tolerance upgrade cost referring to different methods for several probability thresholds (T_D), for the Interoute network.

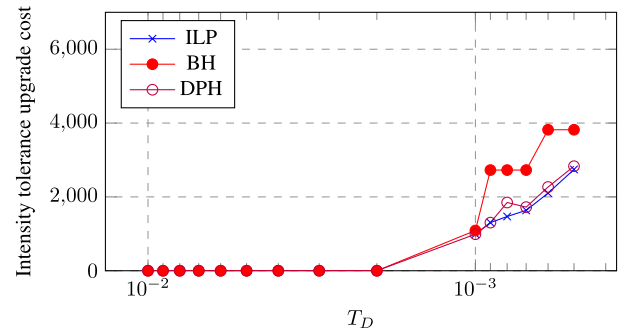**(a)** without availability upgrade (i.e., without the spine)

(b) with availability upgrade (i.e., with the spine)

FIGURE 10. Comparison of the intensity tolerance upgrade cost referring to different methods for several probability thresholds (T_D), for the janos-us network.

intensity tolerance upgrade cost) one, provided by the ILP. Note that $T_D = 1$ means that no disaster resilience upgrade was performed. The utilization of the spine upgrade method significantly increases the average availability of both routing methods. Surprisingly the GDP-R benefits more from this upgrade than the DR scheme, if we look at the absolute increase of the average availability of the connections. Nevertheless, the relative unavailability decrease is slightly higher in the case of the DR method (30%) than in the case of the GDP-R approach (29%).

2) COMPARISON OF GDP-R AND DR METHODS

One benefit of the GDP-R routing method was already presented in Section VII-C, where it was shown that it offers a significantly lower blocking probability than the SRLG Diverse Routing approach. In this section, the focus is on the average availability and average capacity usage of the routing algorithms (i.e., the scenarios where blocking occurs, regardless of the used routing methods, are not included). Table 9 presents the results for different disconnection probability (T_D) values and SRLG probability (T_S) thresholds in the case of two earthquake resilience upgrade methods. The left part of Table 9 corresponds to the DPH method, while its right part corresponds to the optimal (i.e., the most cost-efficient) intensity tolerance upgrade (i.e., based on the ILP). Each

TABLE 8. Availability comparison for the non-blocking scenarios (without and with availability upgrade (spine) to guarantee a minimal target availability $\overline{a_{WP}} = 0.995$) for the Interoute network, using the ILP as the intensity tolerance upgrade method.

T_D	T_S	Average Availability (without the spine)		Average Availability (with the spine)		Number of SRLGs
		DR	GDP-R	DR	GDP-R	
1	0.01	0.997160	0.995840	0.997952	0.996956	10
	0.005	0.998499	0.997104	0.998874	0.997809	16
0.01	0.01	0.996760	0.995433	0.997606	0.996544	6
	0.005	0.997429	0.996200	0.998164	0.997237	11
0.005	0.01	0.996760	0.995433	0.997606	0.996544	6
	0.005	0.997429	0.996200	0.998164	0.997237	11
	0.001	0.999536	0.999297	0.999729	0.999583	36
0.001	0.01	0.996760	0.995433	0.997606	0.996544	6
	0.005	0.997292	0.995989	0.998085	0.997150	9
	0.001	0.999031	0.998341	0.999394	0.998916	24
	0.0005	0.999627	0.999490	0.999770	0.999686	31
0.0005	0.01	0.996760	0.995433	0.997606	0.996544	6
	0.005	0.997089	0.995422	0.997897	0.996586	8
	0.001	0.999119	0.998593	0.999443	0.999069	28
	0.0005	0.999559	0.999482	0.999687	0.999633	36

combination of disconnection probability threshold, SRLG probability threshold and intensity tolerance upgrade method determines an updated network and an SRLG list, which are the input of the routing algorithms. For both intensity tolerance upgrade methods, the corresponding upgrade cost, the number of SRLGs with a probability above T_S, the aver-
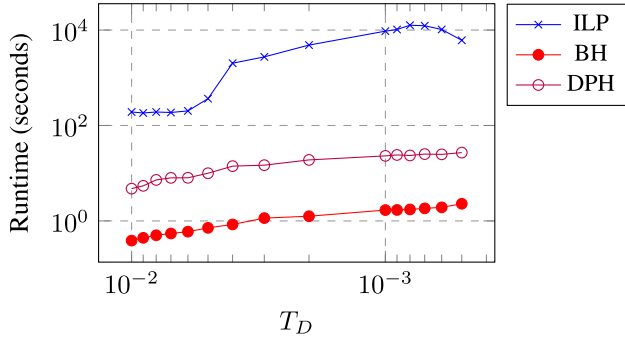
FIGURE 11. Comparison of the computation time values of the three intensity tolerance upgrade methods for different probability thresholds (T_D) for the Interoute network.

FIGURE 12. Comparison of the computation time values of the DPH upgrade method for different networks and probability thresholds (T_D). For each network the upgrade is computed for 10 T_D values.

age availabilities of the two routing methods and their average used capacities are presented.

The first observation is that the average capacity usage of the GDP-R is much lower in most cases compared to the DR scheme. This can be explained by the fact that GDP-R is a more flexible routing method [53], [54] and minimizes the used capacity of the routing while protecting against all failures in the SRLG list. For example, at $T_S = 0.0005$ the SRLG lists are longer. Therefore a more complex routing is needed, and because of that, the difference in average capacity usage will decrease. Note that as the failure scenarios become even more complex, we get to the scenario discussed in Section VII-C, i.e., the DR method will start to block the connections.

The second aspect that catches attention is a slight difference in the average availability in favour of the DR method. In most cases, the short SRLG lists are allowing the GDP-R to use only a single working path for some parts of the route, resulting in a lower average availability. Note that this gap diminishes as the length (i.e., complexity) of the SRLG list is increasing.

The third aspect is related to the difference between the routing results of the two upgrade methods. In most cases, the provided upgrades are similar enough to lead to the same SRLG list. At lower T_D and T_S values, we can observe a slight difference in the number of SRLGs, leading to different routing solutions. In one case, the DPH solution has a higher SRLG count, while in two other cases, the optimal solution does. In these cases, the longer SRLG list causes the increased capacity usage and greater average availability.

Nonetheless, the intensity tolerance upgrade methods (whether ILP or DPH) do not significantly impact the routing results, proving the effectiveness of the heuristic approach again.

F. RUNTIME AND SCALABILITY ANALYSIS OF THE PROPOSED METHODS

In this subsection, we present the runtime and scalability analysis of the spine calculation and the disaster-resilient network planning methods. In addition to the Interoute and
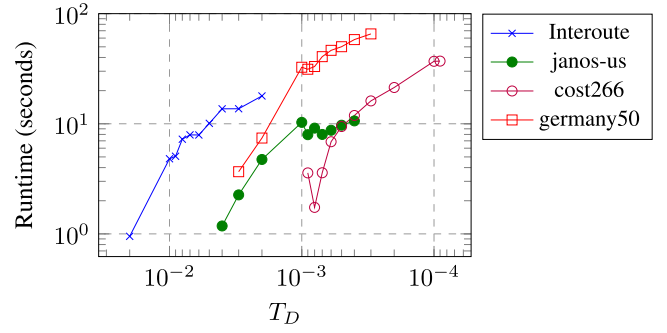
janos-us networks, we used two larger networks too, namely the cost266 (with 37 nodes and 57 edges) and germany50 (with 50 nodes and 88 edges), to show the benefits of our algorithms.

The methods devised for the spine calculation (Algorithm 1 and MILP) have low running times, in the order of minutes. Experiments were run using a Dell Precision 7500 with Intel(R) Xeon(R) CPU X5660 (Six Core, 2.80GHz, 6.4GT/s, 12MB), with 48GB of RAM, using CPLEX 12.5 [89] to solve the MILP. As an example, for the smaller network (Interoute), the heuristic takes about 8 minutes to run and the MILP about 1.3 s per spine. For more sparse networks, the heuristic calculates more spines, due to the increased difficulty in finding spines without unprotected paths. As for the larger network (germany50), the heuristic takes 2.5 minutes and the MILP about 18.0 s per spine.

The computation times of the disaster-resilient network upgrade methods in case of the Interoute network are presented in Fig. 11. We can observe that the runtimes of the heuristic algorithms are negligible compared to the ILP. As expected, the BH method takes the least amount of time to produce a solution (always less than 5 seconds). The DPH algorithm requires more time. However, even at the lowest T_D values, it returns solutions in less than one minute. The ILP runtime varies between a few minutes and a few hours, because of the large number of variables and constraints. For example, in the case of the Interoute network, the ILP input data matrix contained over 16 million rows and over 10 million columns. The running time scales quite well with T_D. However note that the resource consumption of the ILP regarding memory does not scale well with the number of links, min-cuts and earthquakes, since the number of variables and constraints increases rapidly (see Section VI-D). Hence for larger networks we recommend the DPH upgrade method.

In Fig. 12 the computation times of the DPH upgrade method are presented for four networks and 10 different T_D values in each network's case. For each network, the first T_D value is the one for which an upgrade is required, i.e., any T_D values before the displayed ones do not require any upgrade,

TABLE 9. Comparison of the routing results in the case of different intensity tolerance upgrade methods for the Interoute network (with availability upgrade (i.e., with the spine) to guarantee a minimal target availability $\widehat{a_{WP}} = 0.995$).

Thresholds		Disconnection-Probability-based Heuristic (DPH)						ILP					
T_D	T_S	Int.Tol. Upg. Cost	Average availability		Average capacity		Number of SRLGs	Int.Tol. Upg. Cost	Average availability		Average capacity		Number of SRLGs
			DR	GDP-R	DR	GDP-R			DR	GDP-R	DR	GDP-R	
0.01	0.01	719	0.997606	0.996544	5.32	4.82	6	687	0.997606	0.996544	5.32	4.82	6
	0.005		0.998164	0.997237	6.01	5.39	11		0.998164	0.997237	6.01	5.39	11
0.005	0.01	1,746	0.997606	0.996544	5.32	4.82	6	1,717	0.997606	0.996544	5.32	4.82	6
	0.005		0.998164	0.997237	6.01	5.39	11		0.998164	0.997237	6.01	5.39	11
	0.001		0.999729	0.999583	10.03	9.97	36		0.999729	0.999583	10.03	9.97	36
0.001	0.01	4,492	0.997606	0.996544	5.32	4.82	6	4,370	0.997606	0.996544	5.32	4.82	6
	0.005		0.998085	0.997150	5.85	5.10	9		0.998085	0.997150	5.85	5.10	9
	0.001		0.999462	0.999066	8.97	8.62	24		0.999394	0.998916	8.97	8.66	24
	0.0005		0.999783	0.999690	10.10	10.06	33		0.999770	0.999686	9.98	9.93	31
0.0005	0.01	5,655	0.997606	0.996544	5.32	4.82	6	5,311	0.997606	0.996544	5.32	4.82	6
	0.005		0.997897	0.996586	5.71	5.00	8		0.997897	0.996586	5.71	5.00	8
	0.001		0.999348	0.998767	8.85	8.46	23		0.999443	0.999069	9.22	9.00	28
	0.0005		0.999669	0.999548	9.56	9.42	29		0.999687	0.999633	10.05	9.97	36

and hence their corresponding computational time is 0. The last T_D value is such that the total disconnection probability is about one tenth of the initial one.

We can observe that the number of nodes and edges have a significant effect on the runtime of the upgrade method (germany50 has the highest computational time). However, other factors affect it as well, like the number of minimal cuts or the number of earthquake epicenters. Last but not least, the probability distribution of the earthquakes and the topology of the network have a major impact on the upgrade process.

In this example, the number of minimal cuts was between 42 and 47 for the Interoute, the cost266 and the germany50 network; however it was only 33 for the janos-us network. This way the main differences between the networks are their node and edge count, their topology and the probability distribution of the earthquakes in that area. The first probability threshold for each network is the one where $T_D < P_D$, meaning that an upgrade is necessary. Additionally, the beginning of the graphs indicates the disconnection probability (P_D) for each network showing that the Interoute network has the highest P_D and the cost266 network has the lowest (this highlights the importance of the seismic properties of the region).

It is clear that the runtime of the DPH upgrade method is in close connection with the node and edge count of the networks. The Interoute and janos-us networks are similar in size and this is reflected in the upgrade method's runtime. The germany50 network is clearly the largest network in our simulation and its runtimes are the longest too. Since its node and edge count is approximately twice as much as the janos-us network's and their P_D values are very close, a head-to-head runtime comparison is appropriate. For the higher T_D values the ratio of the runtimes is approximately two, but for lower T_D values its between three and six. In accordance with its size, the computation times in case of the cost266 network are higher than in case of the Interoute network and lower than in case of the germany50 network.

In summary, we can state that the computational time and scalability depend on various factors, most of all from the size of the network, the topology and the probability distribution of the earthquakes i.e., the seismic properties of the region.

In this section, we presented several aspects of the experimental results. We demonstrated the benefits of the spine, the disaster-resilient network design and the GDP-R routing. We showed that the DPH method performs well. In terms of cost efficiency of intensity tolerance upgrade, DPH on average is within 5% of the optimal solution, i.e., the solution provided by the ILP. In running time and resource consumption (regarding RAM size), it outperforms the ILP significantly (it is $10 - 100$ times faster and uses about 40 times less RAM).

VIII. CONCLUSION

In our paper, we presented a refined and enhanced version of FRADIR, i.e., the eFRADIR. To make the framework more precise, we incorporated into FRADIR the use of an earthquake activity and magnitude-based failure model yielding a more precise and comprehensive model compared to the most commonly used ground-shaking hazard models. Furthermore, compared to the former versions of FRADIR, in eFRADIR we improved the coupling of the independent random failures and regional failures.

An enhanced spine selection approach was also introduced in eFRADIR allowing to obtain the results in a short time for large networks overcoming a major limitation of FRADIR and FRADIR-II. In particular, the scheme presented in this paper is a two-stage approach, where in the first stage an adaptation of previous heuristics is considered. In addition, we proposed a novel Integer Linear Program for the disaster-resilient network planning for optimal link intensity tolerance upgrades and presented two heuristic schemes to reduce the running time. We have shown that the disconnection-probability-based heuristic method (i.e., DPH) for upgrading the intensity tolerance of the edges, performs really well.

Furthermore, with thorough simulations, we presented the merits of the refined eFRADIR framework for earthquake resilience in two topologies with different scales. In particular, we demonstrated the benefits of the spine, the disaster-resilient network design and the GDP-R routing independently and jointly as building blocks of eFRADIR.

REFERENCES

[1] J. Tapolcai, P. Cholda, T. Cinkler, K. Wajda, A. Jajszczyk, A. Autenrieth, S. Bodamer, D. Colle, G. Ferraris, H. Lonsethagen, I.-E. Svinnset, and D. Verchere, "Quality of resilience (QoR): Nobel approach to the multi-service resilience characterization," in *Proc. 2nd Int. Conf. Broadband Netw.*, Oct. 2005, pp. 1328–1337.

[2] P. Chołda, J. Tapolcai, T. Cinkler, K. Wajda, and A. Jajszczyk, "Quality of resilience QoR as a network reliability characterization tool," *IEEE Network*, vol. 23, no. 2, pp. 11–19, March/Apr. 2009.

[3] J. Tapolcai, P. Chołda, T. Cinkler, K. Wajda, A. Jajszczyk, and D. Verchere, "Quantification of resilience and quality of service," in *Proc. IEEE Int. Conf. Commun. (ICC)*, Istanbul, Turkey, Jun. 2006, pp. 477–482.

[4] J. Rak and D. Hutchison, *Guide to Disaster Resilient Communication Networks*. Cham, Switzerland: Springer, 2020.

[5] Y. Liu, D. Tipper, and P. Siripongwutikorn, "Approximating optimal spare capacity allocation by successive survivable routing," in *Proc. IEEE INFOCOM Conf. Comput. Commun., 20th Annu. Joint Conf. IEEE Comput. Commun. Soc.*, Apr. 2001, pp. 699–708.

[6] V. Y. Liu and D. Tipper, "Spare capacity allocation using shared backup path protection for dual link failures," *Comput. Commun.*, vol. 36, no. 6, pp. 666–677, Mar. 2013.

[7] A. Pašić, R. Girão-Silva, B. Vass, T. Gomes, F. Mogyorósi, P. Babarczi, and J. Tapolcai, "FRADIR-II: An improved framework for disaster resilience," in *Proc. 11th Int. Workshop Resilient Netw. Design Model. (RNDM)*, Oct. 2019, pp. 1–7.

[8] T. Gomes, J. Tapolcai, C. Esposito, D. Hutchison, F. Kuipers, J. Rak, A. de Sousa, A. Iossifides, R. Travanca, J. André, L. Jorge, L. Martins, P. O. Ugalde, A. Pašić, D. Pezaros, S. Jouet, S. Secci, and M. Tornatore, "A survey of strategies for communication networks to protect against large-scale natural disasters," in *Proc. 8th Int. Workshop Resilient Netw. Design Model. (RNDM)*, Sep. 2016, pp. 11–22.

[9] J. Rak, D. Hutchison, E. Calle, T. Gomes, M. Gunkel, P. Smith, J. Tapolcai, S. Verbrugge, and L. Wosinska, "RECODIS: Resilient communication services protecting end-user applications from disaster-based failures," in *Proc. 18th Int. Conf. Transparent Opt. Netw. (ICTON)*, Jul. 2016, pp. 1–4.

[10] A. Mauthe, D. Hutchison, E. K. Çetinkaya, I. Ganchev, J. Rak, J. P. G. Sterbenz, M. Gunkelk, P. Smith, and T. Gomes, "Disaster-resilient communication networks: Principles and best practices," in *Proc. 8th Int. Workshop Resilient Netw. Design Modeling (RNDM)*, Sep. 2016, pp. 1–10.

[11] S. Neumayer, G. Zussman, R. Cohen, and E. Modiano, "Assessing the vulnerability of the fiber infrastructure to disasters," *IEEE/ACM Trans. Netw.*, vol. 19, no. 6, pp. 1610–1623, Dec. 2011.

[12] B. Mukherjee, M. F. Habib, and F. Dikbiyik, "Network adaptability from disaster disruptions and cascading failures," *IEEE Commun. Mag.*, vol. 52, no. 5, pp. 230–238, May 2014.

[13] R. S. Couto, S. Secci, M. M. Campista, and L. M. K. Costa, "Network design requirements for disaster resilience in IaaS clouds," *IEEE Commun. Mag.*, vol. 52, no. 10, pp. 52–58, Oct. 2014.

[14] A. Pašić, R. Girão-Silva, B. Vass, T. Gomes, and P. Babarczi, "FRADIR: A novel framework for disaster resilience," in *Proc. 10th Int. Workshop Resilient Netw. Design Modeling (RNDM)*, Aug. 2018, pp. 1–7.

[15] N. Araki, "ICT standardization trends for disaster relief, network resilience, and recovery by ITU-T," *NTT Tech. Rev.*, vol. 16, no. 10, pp. 77–82, Oct. 2018.

[16] J. Tapolcai, B. Vass, Z. Heszberger, J. Biró, D. Hay, F. A. Kuipers, and L. Rónyai, "A tractable stochastic model of correlated link failures caused by disasters," in *Proc. IEEE INFOCOM Conf. Comput. Commun.*, Apr. 2018, pp. 2105–2113.

[17] P. Babarczi, G. Biczók, H. Øverby, J. Tapolcai, and P. Soproni, "Realization strategies of dedicated path protection: A bandwidth cost perspective," *Comput. Netw.*, vol. 57, no. 9, pp. 1974–1990, Jun. 2013.

[18] R. Goścień, K. Walkowiak, M. Klinkowski, and J. Rak, "Protection in elastic optical networks," *IEEE Netw.*, vol. 29, no. 6, pp. 88–96, Nov./Dec. 2015.

[19] A. Kwasinski, W. W. Weaver, P. L. Chapman, and P. T. Krein, "Telecommunications power plant damage assessment for Hurricane Katrina—Site survey and follow-up results," *IEEE Syst. J.*, vol. 3, no. 3, pp. 277–287, Aug. 2009.

[20] W. Wu, B. Moran, J. H. Manton, and M. Zukerman, "Topology design of undersea cables considering survivability under major disasters," in *Proc. Int. Conf. Adv. Inf. Netw. Appl. Workshops*, May 2009, pp. 1154–1159.

[21] M. F. Habib, M. Tornatore, F. Dikbiyik, and B. Mukherjee, "Disaster survivability in optical communication networks," *Comput. Commun.*, vol. 36, no. 6, pp. 630–644, Mar. 2013.

[22] F. Dikbiyik, M. Tornatore, and B. Mukherjee, "Minimizing the risk from disaster failures in optical backbone networks," *J. Lightw. Technol.*, vol. 32, no. 18, pp. 3175–3183, Sep. 15, 2014.

[23] (Aug. 2018). *Atlantic Hurricane Season Impact on Communications—Report and Recommendations—Public Safety Docket No. 17–344.* Public Safety and Homeland Security Bureau—Federal Communications Commission (FCC). [Online]. Available: https://docs.fcc.gov/public/attachments/DOC-353805A1.pdf

[24] G. Xanthopoulos and M. Athanasiou, "Attica region, Greece July 2018: A tale of two fires and a seaside tragedy," *Wildfire*, vol. 28, no. 2, pp. 18–21, Apr. 2019.

[25] (2020). *Cyclone Amphan: Telecom Networks Operating at 65-70% Capacity in Affected Districts, Says COAI.* Deccan Herald News. [Online]. Available: https://www.deccanherald.com/national/east-and-northeast/cyclone-amphan-telecom-networks-operating-at-65-70-capacity-in-affected-districts-says-coai-840844.html

[26] C. Mas Machuca, S. Secci, P. Vizarreta, F. Kuipers, A. Gouglidis, D. Hutchison, S. Jouet, D. Pezaros, A. Elmokashfi, P. Heegaard, S. Ristov, and M. Gusev, "Technology-related disasters: A survey towards disaster-resilient software defined networks," in *Proc. 8th Int. Workshop Resilient Netw. Design Modeling (RNDM)*, Sep. 2016, pp. 35–42.

[27] J. Svetlik. (Aug. 2013). *Google Goes Down for 5 Minutes, Internet Traffic Drops 40%.* CNET. [Online]. Available: https://www.cnet.com/news/google-goes-down-for-5-minutes-internet-traffic-drops-40/

[28] (2017). *Summary of the Amazon S3 Service Disruption in the Northern Virginia (US-EAST-1) Region.* [Online]. Available: https://aws.amazon.com/message/41926/

[29] (2019). *Azure Status History.* Microsoft Azure. [Online]. Available: https://azure.microsoft.com//status/history/

[30] J. S. Foster, E. Gjelde, W. R. Graham, R. J. Hermann, H. M. Kluepfel, R. L. Lawson, G. K. Soper, L. L. Wood, and J. B. Woodard, "Report of the commission to assess the threat to the United States from electromagnetic pulse (EMP) attack. Volume 1: Executive report," EMP Commission, New York, NY, USA, Tech. Rep., 2008.

[31] P. Nicholson. (Jul. 2020). *Five Most Famous DDoS Attacks and Then Some.* A10 Blog. [Online]. Available: https://www.a10networks.com/blog/5-most-famous-ddos-attacks/

[32] J. Rak, D. Hutchison, J. Tapolcai, R. Bruzgiene, M. Tornatore, C. Mas-Machuca, M. Furdek, and P. Smith, "Fundamentals of communication networks resilience to disasters and massive disruptions," in *Guide to Disaster Resilient Communication Networks*, J. Rak and D. Hutchison, Eds. Cham, Switzerland: Springer, 2020, ch. 1, pp. 1–43.

[33] O. Gerstel, M. Jinno, A. Lord, and S. J. Yoo, "Elastic optical networking: A new dawn for the optical layer?" *IEEE Commun. Mag.*, vol. 50, no. 2, pp. s12–s20, Feb. 2012.

[34] M. F. Habib, M. Tornatore, M. De Leenheer, F. Dikbiyik, and B. Mukherjee, "Design of disaster-resilient optical datacenter networks," *J. Lightw. Technol.*, vol. 30, no. 16, pp. 2563–2573, Aug. 2012.

[35] J. Heidemann, L. Quan, and Y. Pradkin, *A Preliminary Analysis of Network Outages During Hurricane Sandy.* Los Angeles, CA, USA: Univ. Southern California, Information Sciences Institute, 2012.

[36] I. B. B. Harter, D. A. Schupke, M. Hoffmann, and G. Carle, "Network virtualization for disaster resilience of cloud services," *IEEE Commun. Mag.*, vol. 52, no. 12, pp. 88–95, Dec. 2014.

[37] X. Long, D. Tipper, and T. Gomes, "Measuring the survivability of networks to geographic correlated failures," *Opt. Switching Netw.*, vol. 14, pp. 117–133, Aug. 2014.

[38] S. Neumayer, A. Efrat, and E. Modiano, "Geographic max-flow and min-cut under a circular disk failure model," *Comput. Netw.*, vol. 77, pp. 117–127, Feb. 2015.

[39] H. Saito, "Spatial design of physical network robust against earthquakes," *J. Lightw. Technol.*, vol. 33, no. 2, pp. 443–458, Jan. 15, 2015.

[40] H. Saito, "Analysis of geometric disaster evaluation model for physical networks," *IEEE/ACM Trans. Netw.*, vol. 23, no. 6, pp. 1777–1789, Dec. 2015.

[41] C. Cao, M. Zukerman, W. Wu, J. H. Manton, and B. Moran, "Survivable topology design of submarine networks," *J. Lightw. Technol.*, vol. 31, no. 5, pp. 715–730, Mar. 2013.

[42] A. Sen, S. Murthy, and S. Banerjee, "Region-based connectivity—A new paradigm for design of fault-tolerant networks," in *Proc. Int. Conf. High Perform. Switching Routing*, Jun. 2009, pp. 1–7.

[43] Y. Awaji, H. Furukawa, S. Xu, M. Shiraiwa, N. Wada, and T. Tsuritani, "Resilient optical network technologies for catastrophic disasters," *J. Opt. Commun. Netw.*, vol. 9, no. 6, pp. A280–A289, 2017.

[44] A. Agrawal, V. Bhatia, and S. Prakash, "Network and risk modeling for disaster survivability analysis of backbone optical communication networks," *J. Lightw. Technol.*, vol. 37, no. 10, pp. 2352–2362, May 15, 2019.

[45] D. Papadimitriou and B. Fortz, "Reliability-dependent combined network design and routing optimization," in *Proc. 6th Int. Workshop Reliable Netw. Design Modeling (RNDM)*, Nov. 2014, pp. 31–38.

[46] B. Elshqeirat, S. Soh, S. Rai, and M. Lazarescu, "Topology design with minimal cost subject to network reliability constraint," *IEEE Trans. Rel.*, vol. 64, no. 1, pp. 118–131, Mar. 2015.

[47] F. Robledo, P. Romero, and M. Saravia, "On the interplay between topological network design and diameter constrained reliability," in *Proc. 12th Int. Conf. Design Reliable Commun. Netw. (DRCN)*, Mar. 2016, pp. 106–108.

[48] Y. Prieto, J. E. Pezoa, N. Boettcher, and S. K. Sobarzo, "Increasing network reliability to correlated failures through optimal multiculture design," in *Proc. CHILEAN Conf. Electr., Electron. Eng., Inf. Commun. Technol. (CHILECON)*, Oct. 2017, pp. 1–6.

[49] D. Tipper, "Resilient network design: Challenges and future directions," *Telecommun. Syst.*, vol. 56, no. 1, pp. 5–16, May 2014.

[50] A. Alashaikh, T. Gomes, and D. Tipper, "The spine concept for improving network availability," *Comput. Netw.*, vol. 82, pp. 4–19, May 2015.

[51] J. Zhang, E. Modiano, and D. Hay, "Enhancing network robustness via shielding," in *Proc. 11th Int. Conf. Design Reliable Commun. Netw. (DRCN)*, Mar. 2015, pp. 17–24.

[52] J. Rak, *Resilient Routing in Communication Networks*. Cham, Switzerland: Springer, 2015.

[53] W. Kellerer, A. Basta, P. Babarczi, A. Blenk, M. He, M. Klügel, and A. M. Alba, "How to measure network flexibility? A proposal for evaluating softwarized networks," *IEEE Commun. Mag.*, vol. 56, no. 10, pp. 186–192, Oct. 2018.

[54] P. Babarczi, M. Klügel, A. M. Alba, M. He, J. Zerwas, P. Kalmbach, A. Blenk, and W. Kellerer, "A mathematical framework for measuring network flexibility," *Comput. Commun.*, vol. 164, pp. 13–24, Dec. 2020.

[55] M. Tornatore, P. Babarczi, O. Ayoub, S. Ferdousi, R. Lourenco, J. Zerwas, A. Blenk, M. Klügel, and W. Kellerer, "Alert-based network reconfiguration and data evacuation," in *Guide to Disaster-resilient Communication Networks*, J. Rak and D. Hutchison, Eds. Cham, Switzerland: Springer, 2020, ch. 14, pp. 353–377.

[56] P. Babarczi, A. Pašić, J. Tapolcai, F. Németh, and B. Ladóczki, "Instantaneous recovery of unicast connections in transport networks: Routing versus coding," *Comput. Netw.*, vol. 82, pp. 68–80, May 2015.

[57] J. Yallouz and A. Orda, "Tunable QoS-aware network survivability," *IEEE/ACM Trans. Netw.*, vol. 25, no. 1, pp. 139–149, Feb. 2017.

[58] S. Rouayheb, A. Sprintson, and C. Georghiades, "Robust network codes for unicast connections: A case study," *IEEE/ACM Trans. Netw.*, vol. 19, no. 3, pp. 644–656, Jun. 2011.

[59] P. Babarczi, J. Tapolcai, A. Pašić, L. Rónyai, E. R. Bérczi-Kovács, and M. Médard, "Diversity coding in two-connected networks," *IEEE/ACM Trans. Netw.*, vol. 25, no. 4, pp. 2308–2319, Aug. 2017.

[60] A. Pašić, P. Babarczi, J. Tapolcai, E. R. Bérczi-Kovács, Z. Király, and L. Rónyai, "Minimum cost survivable routing algorithms for generalized diversity coding," *IEEE/ACM Trans. Netw.*, vol. 28, no. 1, pp. 289–300, Feb. 2020.

[61] Y. Cheng, D. Medhi, and J. P. G. Sterbenz, "Geodiverse routing with path delay and skew requirement under area-based challenges," *Networks*, vol. 66, no. 4, pp. 335–346, Dec. 2015.

[62] A. de Sousa, D. Santos, and P. Monteiro, "Determination of the minimum cost pair of *D*-geodiverse paths," in *Proc. Int. Conf. Design Reliable Commun. Netw. (DRCN)*, Mar. 2017, pp. 1–8.

[63] M. W. Ashraf, S. M. Idrus, F. Iqbal, and R. A. Butt, "On spatially disjoint lightpaths in optical networks," *Photonic Netw. Commun.*, vol. 36, no. 1, pp. 11–25, Aug. 2018.

[64] S. Verbrugge, D. Colle, P. Demeester, R. Huelsermann, and M. Jaeger, "General availability model for multilayer transport networks," in *Proc. 5th Int. Workshop Design Reliable Commun. Netw., DRCN*, Oct. 2005, p. 8.

[65] L. Pašić, A. Pašić, F. Mogyorósi, and A. Pašić, "FRADIR meets availability," in *Proc. 16th Int. Conf. Design Reliable Commun. Netw. DRCN*, Mar. 2020, pp. 1–6.

[66] J. Q. Hu, "Diverse routing in optical mesh networks," *IEEE Trans. Commun.*, vol. 51, no. 3, pp. 489–494, Mar. 2003.

[67] P. Cholda and A. Jajszczyk, "Recovery and its quality in multilayer networks," *J. Lightw. Technol.*, vol. 28, no. 4, pp. 372–389, Feb. 2010.

[68] S. Ramamurthy, L. Sahasrabuddhe, and B. Mukherjee, "Survivable WDM mesh networks," *J. Lightw. Technol.*, vol. 21, no. 4, pp. 870–883, Apr. 2003.

[69] M. Klinkowski, P. Lechowicz, and K. Walkowiak, "Survey of resource allocation schemes and algorithms in spectrally-spatially flexible optical networking," *Opt. Switching Netw.*, vol. 27, pp. 58–78, Jan. 2018.

[70] A. Alashaikh, D. Tipper, and T. Gomes, "Embedded network design to support availability differentiation," *Ann. Telecommun.*, vol. 74, nos. 9–10, pp. 605–623, Oct. 2019.

[71] R. Girão-Silva, L. Martins, T. Gomes, D. Tipper, and A. Alashaikh, "Heuristic approach for the design of a high availability structure," in *Proc. 15th Int. Conf. Design Reliable Commun. Netw. (DRCN)*, Mar. 2019, pp. 29–36.

[72] R. Girão-Silva, T. Gomes, L. Martins, D. Tipper, and A. Alashaikh, "A centrality-based heuristic for network design to support availability differentiation," in *Proc. 16th Int. Conf. Design Reliable Commun. Netw. DRCN*, Mar. 2020, pp. 1–7.

[73] K. Jiang, D. Ediger, and D. A. Bader, "Generalizing k-betweenness centrality using short paths and a parallel multithreaded implementation," in *Proc. Int. Conf. Parallel Process.*, Sep. 2009, pp. 542–549.

[74] Y. Rochat, "Closeness centrality extended to unconnected graphs: The harmonic centrality index," in *Proc. 6th Appl. Social Netw. Anal. Conf. (ASNA)*, Zürich, Switzerland, Aug. 2009, pp. 1–15.

[75] R. C. Prim, "Shortest connection networks and some generalizations," *Bell Syst. Tech. J.*, vol. 36, no. 6, pp. 1389–1401, Nov. 1957.

[76] B. Vass, J. Tapolcai, D. Hay, J. Oostenbrink, and F. Kuipers, "How to model and enumerate geographically correlated failure events in communication networks," in *Guide to Disaster-Resilient Communication Networks*, J. Rak and D. Hutchison, Eds. Cham, Switzerland: Springer, 2020, ch. 4, pp. 87–115.

[77] P. K. Agarwal, A. Efrat, S. K. Ganjugunte, D. Hay, S. Sankararaman, and G. Zussman, "The resilience of WDM networks to probabilistic geographical failures," *IEEE/ACM Trans. Netw.*, vol. 21, no. 5, pp. 1525–1538, Oct. 2013.

[78] P. N. Tran and H. Saito, "Geographical route design of physical networks using earthquake risk information," *IEEE Commun. Mag.*, vol. 54, no. 7, pp. 131–137, Jul. 2016.

[79] H. Honda and H. Saito, "Nation-wide disaster avoidance control against heavy rain," *IEEE/ACM Trans. Netw.*, vol. 27, no. 3, pp. 1084–1097, Jun. 2019.

[80] A. Valentini, B. Vass, J. Oostenbrink, L. Csak, F. Kuipers, B. Pace, D. Hay, and J. Tapolcai, "Network resiliency against Earthquakes," in *Proc. 11th Int. Workshop Resilient Netw. Design Modeling (RNDM)*, Oct. 2019, pp. 1–7.

[81] A. Rovida, M. Locati, R. Camassi, B. Lolli, and P. Gasperini, Eds., *Italian Parametric Earthquake Catalogue (CPTI15)*. Istituto Nazionale di Geofisica e Vulcanologia (INGV), 2016. [Online]. Available: https://emidius.mi.ingv.it/CPTI15-DBMI15_v1.5/description_CPTI15_en.htm, doi: 10.6092/INGV.IT-CPTI15.

[82] C. S. Mueller, "Earthquake catalogs for the USGS national seismic hazard maps," *Seismological Res. Lett.*, vol. 90, no. 1, pp. 251–261, Jan. 2019.

[83] D. Giardini *et al.*, "Seismic hazard harmonization in Europe (SHARE): Online data resource," SHARE—Seismic Hazard Harmonization Eur., Zürich, Switzerland, Tech. Rep., 2013. [Online]. Available: http://www.share-eu.org/, doi: 10.12686/SED-00000001-SHARE.

[84] C. Pasolini, D. Albarello, P. Gasperini, V. D'Amico, and B. Lolli, "The attenuation of seismic intensity in italy, part II: Modeling and validation," *Bull. Seismolog. Soc. Amer.*, vol. 98, no. 2, pp. 692–708, Apr. 2008.

[85] W. H. Bakun, "MMI attenuation and historical earthquakes in the basin and range province of western north america," *Bull. Seismolog. Soc. Amer.*, vol. 96, no. 6, pp. 2206–2220, Dec. 2006.

[86] S. Orlowski, R. Wessäly, M. Pióro, and A. Tomaszewski, "SNDlib 1.0–Survivable Network Design library," *Networks*, vol. 55, no. 3, pp. 276–286, 2010. [Online]. Available: http://sndlib.zib.de.

[87] (2020). *Gurobi Optimizer Reference Manual*. Gurobi Optimization, LLC. [Online]. Available: http://www.gurobi.com

[88] D. R. Shier, *Network Reliability and Algebraic Structures*. Oxford, U.K.: Clarendon Press, 1991.

[89] *IBM ILOG CPLEX Optimization Studio V12.5*, IBM, New York, NY, USA, 2012.

ALIJA PAŠIĆ received the M.Sc. *(summa cum laude)* and Ph.D. *(summa cum laude)* degrees in electrical engineering from the Budapest University of Technology and Economics (BME), Hungary, in 2013 and 2019, respectively. He is currently an Assistant Professor with the High-Speed Networks Laboratory, Department of Telecommunications and Media Informatics, BME. His research interests include survivability in optical backbone networks, network coding, machine learning, artificial intelligence (AI), and mobile positioning.

RITA GIRÃO-SILVA received the Ph.D. degree in electrical engineering (telecommunications and electronics) from the University of Coimbra, in 2009. She is currently an Assistant Professor with the Department of Electrical and Computer Engineering, University of Coimbra, and a Researcher with the Institute for Systems Engineering and Computers, Coimbra (INESC Coimbra). Her research interests include routing models, network reliability, and network flow models for routing in telecommunications networks, as well as applications of operational research techniques to problems in telecommunication networks. She has participated in different research and development projects, including projects of cooperation between the university and industry.

FERENC MOGYORÓSI (Member, IEEE) received the M.Sc. degree *(summa cum laude)* in electrical engineering from the Budapest University of Technology and Economics (BME), Hungary, in 2020. He is currently pursuing the Ph.D. degree with the High-Speed Networks Laboratory, Department of Telecommunications and Media Informatics, with the Doctoral School of Electrical Engineering, BME. His research interests include survivability in optical backbone networks, artificial intelligence (AI), and mobile positioning.

BALÁZS VASS (Graduate Student Member, IEEE) received the M.Sc. degree in applied mathematics with Eötvös Loránd Science University (ELTE), Budapest, in 2016, and the Ph.D. degree in informatics from the Budapest University of Technology and Economics (BME), in 2016. His research interests include networking, survivability, combinatorial optimization, and graph theory. He received the Best Paper Award of NaNa'16, and the Best-in-Session Presentation award on INFOCOM'18. He was an invited Speaker of COST RECODIS Training School on Design of Disaster-resilient Communication Networks, in 2019.

TERESA GOMES (Member, IEEE) received the Ph.D. degree in electrical engineering (telecommunications and electronics) from the University of Coimbra, in 1998. She has been an Assistant Professor with the Department of Electrical and Computer Engineering, University of Coimbra, since 1998, and has been with the permanent position since 2003. From April 2013 until July 2013, she was a Visiting Researcher with the School of Information Sciences, University of Pittsburgh, Pittsburgh, PA, USA. She is currently a Researcher with the Institute for Systems Engineering and Computers, Coimbra, (INESC Coimbra). She is the author or coauthor of more than 90 technical publications in international journals, conference proceedings, and book chapters, including one European patent. Her main research interests include routing, protection and reliability analysis models, and algorithms for communication networks. She has been responsible for several national projects, mainly with industry. She has also served as a TPC Member for numerous international conferences and was the Co-Chair for DRCN 2019. She is an Associate Editor of the *Journal of Network and Systems Management* (Springer).

PÉTER BABARCZI (Member, IEEE) received the M.Sc. and Ph.D. degrees *(summa cum laude)* in computer science from the Budapest University of Technology and Economics (BME), Hungary, in 2008 and 2012, respectively. From 2017 to 2019, he was an Alexander von Humboldt Postdoctoral Research Fellow with the Chair of Communication Networks with the Technical University of Munich, Germany. He is currently working as an Assistant Professor with the Department of Telecommunications and Media Informatics, BME. His current research interests include intelligent self-driving networks, the multi-path Internet routing, network coding in transport networks, and combinatorial optimization in softwarized networks. He received the János Bolyai Research Scholarship of the Hungarian Academy of Sciences, in 2013, the Post-doctoral Research Fellowship of the Alexander von Humboldt Foundation, in 2017. Since 2020, he has been the Lead Researcher of an OTKA FK Young Researchers' Excellence Programme supported by the National Research, Development, and Innovation Fund of Hungary.

PÉTER REVISNYEI received the B.Sc. degree in biology from Eötvös Loránd University (ELTE), Hungary, in 2018, and the M.Sc. degree in biomedical engineering from the Budapest University of Technology and Economics (BME), Hungary, in 2020. His research interests include sport analytics and machine learning.

JÁNOS TAPOLCAI received the M.Sc. degree in technical informatics and the Ph.D. degree in computer science from the Budapest University of Technology and Economics (BME), Budapest, in 2000 and 2005, respectively, and the D.Sc. degree in engineering science from the Hungarian Academy of Sciences (MTA), in 2013.

He is currently a Full Professor with the High-Speed Networks Laboratory, Department of Telecommunications and Media Informatics, BME. He has authored more than 150 scientific publications. He was a recipient of several Best Paper awards, including ICC'06, DRCN'11, HPSR'15, and NaNa'16. He is a Winner of the MTA Lendület Program and the Google Faculty Award in 2012 and the Microsoft Azure Research Award in 2018. He is a TPC Member of leading conferences, e.g., IEEE INFOCOM 2012-, and the General Chair of ACM SIGCOMM 2018.

JACEK RAK (Senior Member, IEEE) received the M.Sc., Ph.D., and D.Sc. degrees *(habilitation)* from the Gdańsk University of Technology, Gdańsk, Poland, in 2003, 2009, and 2016, respectively.

He is currently an Associate Professor and the Head of the Department of Computer Communications, Gdańsk University of Technology. He has authored more than 100 publications, including the book *Resilient Routing in Communication Networks* (Springer, 2015). His main research interests include the resilience of communication networks and networked systems. From 2016 to 2020, he was leading the COST CA15127 Action Resilient Communication Services Protecting End-user Applications from Disaster-based Failures (RECODIS) involving more than 170 members from 31 countries. He has also served as a TPC Member for numerous conferences and journals. Recently, he has been the General Chair of ITS-T'17 and MMM-ACNS'17, the General Co-Chair of NETWORKS'16, the TPC Chair of ONDM'17, and the TPC Co-Chair of IFIP Networking'19. He is A Member of the Editorial Board of Optical Switching and Networking, Elsevier and the founder of the International Workshop on Resilient Networks Design and Modeling (RNDM).

● ● ●